SUPPLEMENTARY DATA

From virtual screening hits targeting a cryptic pocket in BACE-1 to a nontoxic brain permeable multitarget anti-Alzheimer lead with disease-modifying and cognition-enhancing effects

Caterina Pont,[1] Tiziana Ginex,[2] Christian Griñán-Ferré,[3] Matthias Scheiner,[4] Alexia Mattellone,[5] Noemí Martínez,[1] Elsa M. Arce,[1] Yolanda Soriano-Fernández,[3] Marina Naldi,[5] Angela De Simone,[6] Marta Barenys,[7] Jesús Gómez-Catalán,[7] Belén Pérez,[8] Raimon Sabate,[9] Vincenza Andrisano,[10] María Isabel Loza,[11] José Brea,[11] Manuela Bartolini,[5] Maria Laura Bolognesi,[5] Michael Decker,[4] Mercè Pallàs,[3] F. Javier Luque,[*,2] Diego Muñoz-Torrero[*,1]

[1] *Laboratory of Medicinal Chemistry (CSIC Associated Unit), Faculty of Pharmacy and Food Sciences, and Institute of Biomedicine (IBUB), University of Barcelona, Av. Joan XXIII 27-31, E-08028 Barcelona, Spain*

[2] *Department of Nutrition, Food Science and Gastronomy, Faculty of Pharmacy and Food Sciences, IBUB, and Institute of Theoretical and Computational Chemistry (IQTC), UB, E-08921 Santa Coloma de Gramenet, Spain*

[3] *Pharmacology Section, Department of Pharmacology, Toxicology and Therapeutic Chemistry, Faculty of Pharmacy and Food Sciences, and Institute of Neuroscience, University of Barcelona, Av. Joan XXIII, 27-31, E-08028, Barcelona, Spain*

[4] *Pharmaceutical and Medicinal Chemistry, Institute of Pharmacy and Food Chemistry, Julius Maximilian University of Würzburg, Am Hubland, DE-97074 Würzburg, Germany*

[5] *Department of Pharmacy and Biotechnology, Alma Mater Studiorum University of Bologna, Via Belmeloro 6, I-40126 Bologna, Italy*

[6] *Department of Drug Science and Technology, University of Turin, I-10125 Torino, Italy*

[7] *GRET, INSA-UB, and Toxicology Unit, Department of Pharmacology, Toxicology and Therapeutic Chemistry, Faculty of Pharmacy and Food Sciences, University of Barcelona, Av. Joan XXIII 27-31, E-08028 Barcelona, Spain*

[8] *Department of Pharmacology, Therapeutics, and Toxicology, Autonomous University of Barcelona, E-08193 Bellaterra, Spain*

[9] *Department of Pharmacy and Pharmaceutical Technology and Physical-Chemistry, Faculty of Pharmacy and Food Sciences, and Institute of Nanoscience and Nanotechnology (IN2UB), University of Barcelona, Av. Joan XXIII 27-31, E-08028 Barcelona, Spain*

[10] *Department for Life Quality Studies, Alma Mater Studiorum University of Bologna, Corso d'Augusto 237, I-47921 Rimini, Italy*

[11] *BioFarma Research Group, Centro Singular de Investigación en Medicina Molecular y Enfermedades Crónicas (CIMUS), Universidade de Santiago de Compostela, Av. de Barcelona s/n, E-15782, Santiago de Compostela, Spain*

* Corresponding authors. Tel.: +34 934033788; E-mail address: fjluque@ub.edu (F.J. Luque); Tel.: +34 934024533; E-mail address: dmunoztorrero@ub.edu (D. Muñoz-Torrero).

TABLE OF CONTENTS

Fig. S1. Results of the two-step virtual screening performed for two BACE-1 structures (model 1 and model 2) S4
Table S1. Chemical structure and score of the potential hits selected after visual inspection of the docking solutions for BACE-1 model-1 S5
Table S2. Chemical structure and score of the potential hits selected after visual inspection of the docking solutions for BACE-1 model-2 S7
Fig. S2. RMSD analysis of protein backbone and ligand for the MD simulated complexes of BACE-1 with compounds **10** and **11** S13
Fig. S3. Distance analysis for selected interactions between compounds **10** and **11** and residues in BACE-1 S14
Fig. S4. Comparison of the simulated complexes of BACE-1 with **11** and **10** with the binding mode found for the complex with the rhein–huprine hybrid **1** S15
In vitro determination of hBACE-1 inhibitory activity S16
In vitro determination of hAChE and hBChE inhibitory activity S17
Determination of the Aβ42 and tau antiaggregating activity in intact *E. coli* cells S18
Fig. S5. UV/vis absorption spectra of the target compounds in the absence and presence of metal salts S19
Table S3. Cu^{2+} chelation ability and antioxidant activity of the target compounds S20
Neuroprotection and neurotoxicity assay in HT22 cells S21
Table S4. Neuroprotective effects of compounds **9**–**12** against glutamate-induced oxidative stress in neuronal HT22 cells S22
Table S5. Neurotoxicity of the target hybrids on neuronal HT22 cells S23
In vitro brain permeability: PAMPA-BBB assay S24
Table S6. PAMPA-BBB permeabilities of commercial drugs for assay validation S25
Molecular analysis. Western blotting S26
Table S7. Antibodies used in Western blot and immunohistochemistry studies S27
RNA extraction and determination of gene expression by q-PCR S28
Table S8. Primers and probes used in qPCR studies S29
Copies of ^{1}H and ^{13}C NMR spectra and HPLC chromatograms of target compounds S30

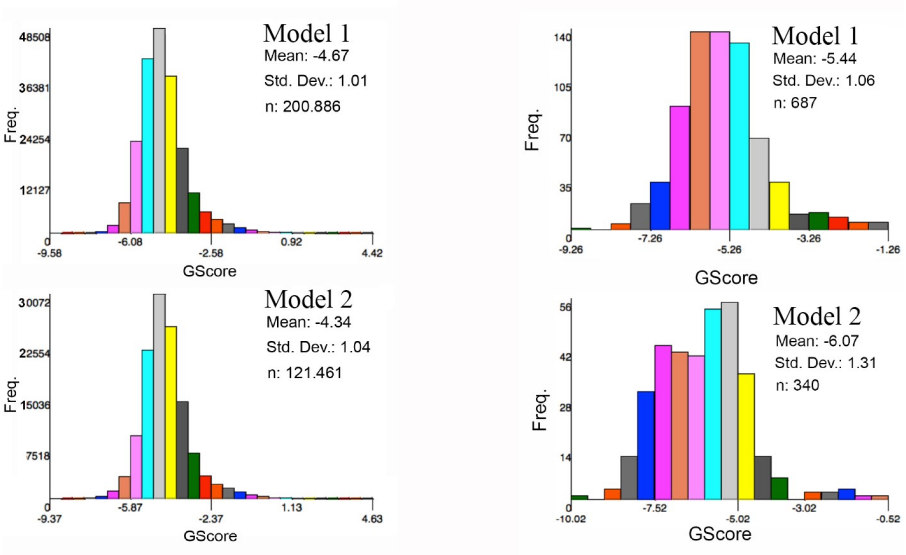

Fig. S1. Results of the two-step virtual screening performed for two BACE-1 structures (model 1 and model 2). (Left) Preliminary virtual screening with HTVS GScore function: Only poses with GScore < –7.0 kcal/mol were retained. (Right) Screening performed with the extra precision (XP) GScore function: Poses with GScore values < –6.5 kcal/mol were finally kept for visual inspection.

Table S1

Chemical structures and scores of the candidates selected after visual inspection of the docking solutions for BACE-1 model-1[a]

Entry	Structure	Score	Entry	Structure	Score
1	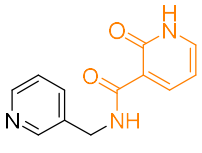	–7.6	**2**	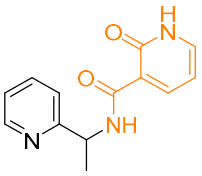	–6.9
3	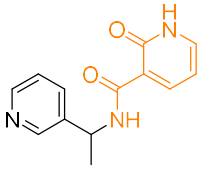	–6.9	**4**	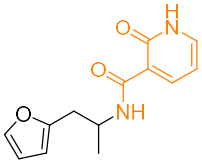	–6.5
5	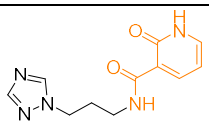	–6.5	**6**	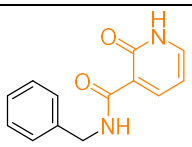	–7.1
7	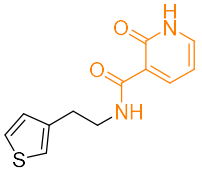	–6.5	**8**	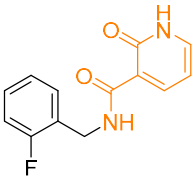	–7.0
9	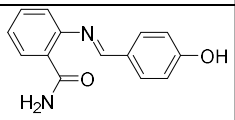	–6.7	**10**	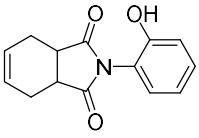	–6.6
11	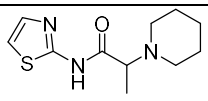	–7.2	**12**	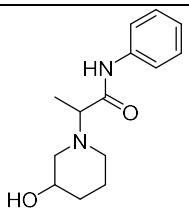	–7.6
13	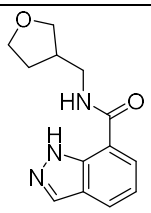	–7.6	**14**	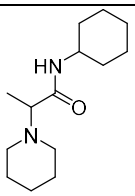	–6.8

15	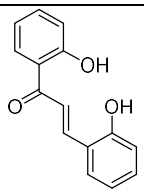	–6.6	**16**	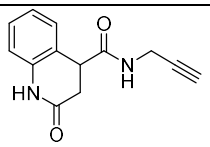	–7.5
17	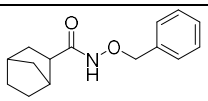	–6.5	**18**	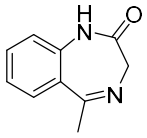	–7.4

[a]The scaffolds of the virtual hits that were selected for the design of the target hybrids are highlighted in colour.

Table S2

Chemical structures and scores of the candidates selected after visual inspection of the docking solutions for BACE-1 model-2[a]

Entry	Structure	Score	Entry	Structure	Score
1	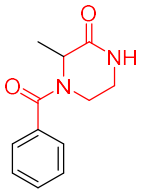	–7.6	**2**	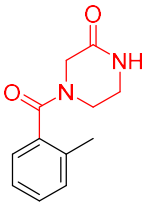	–7.8
3	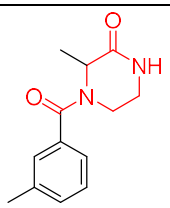	–8.0	**4**	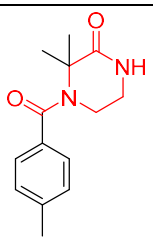	–6.8
5	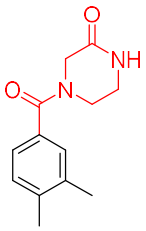	–8.2	**6**	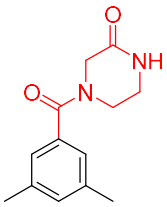	–8.2
7	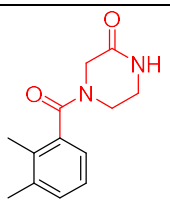	–7.0	**8**	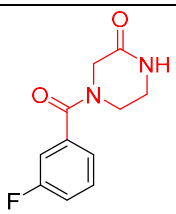	–6.9
9	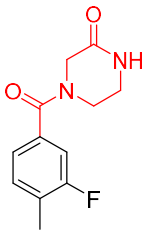	–8.0	**10**	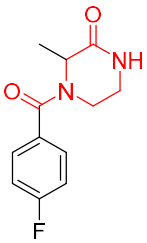	–7.1

11	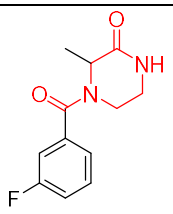	−7.8	**12**	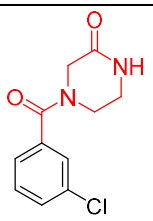	−7.9
13	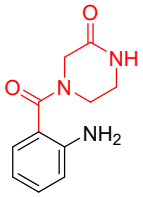	−7.7	**14**	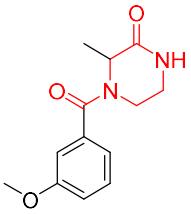	−7.4
15	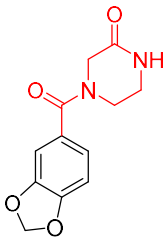	−8.0	**16**	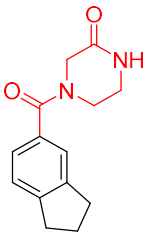	−8.3
17	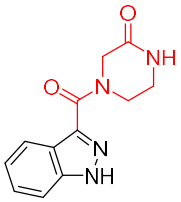	−7.0	**18**	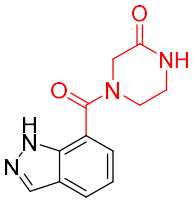	−7.3
19	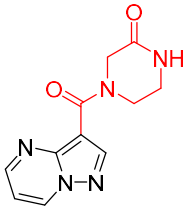	−7.6	**20**	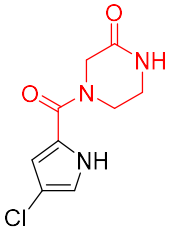	−7.0
21	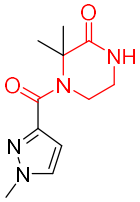	−7.6	**22**	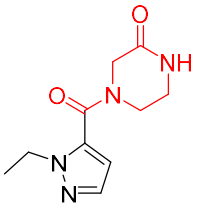	−7.7
23	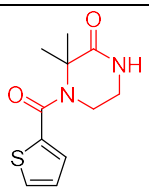	−7.3	**24**	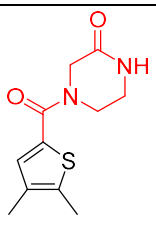	−7.9

25	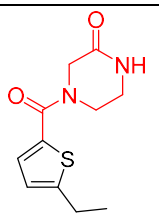	−7.1	**26**	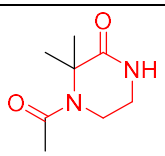	−7.4
27	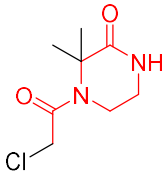	−7.4	**28**	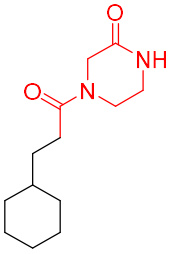	−7.1
29	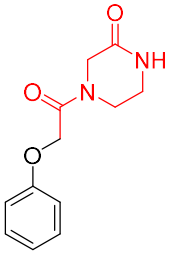	−7.4	**30**	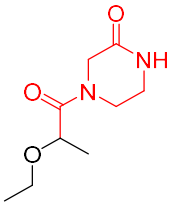	−7.0
31	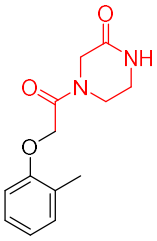	−7.5	**32**	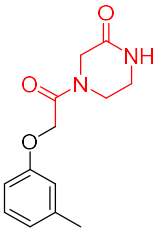	−7.4
33	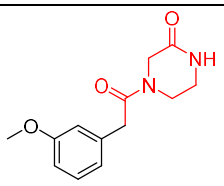	−8.3	**34**	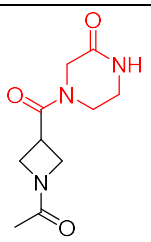	−6.5
35	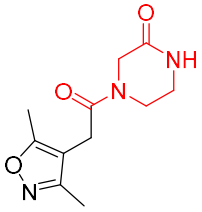	−7.2	**36**	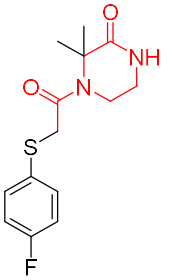	−7.1

37	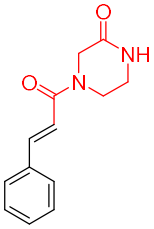	−7.0	**38**	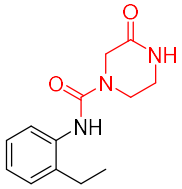	−7.9
39	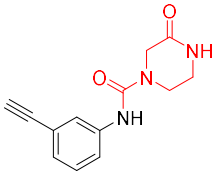	−8.6	**40**	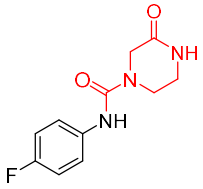	−7.7
41	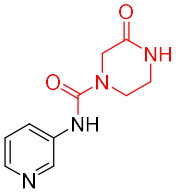	−8.0	**42**	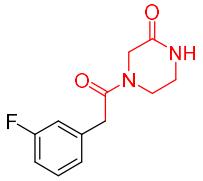	−6.9
43	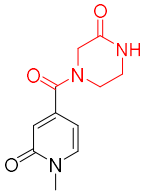	−7.3	**44**	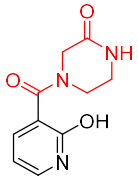	−7.1
45	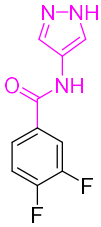	−7.2	**46**	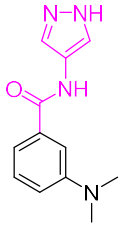	−8.0
47	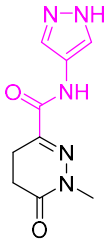	−7.5	**48**	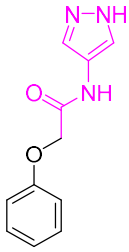	−7.5

49	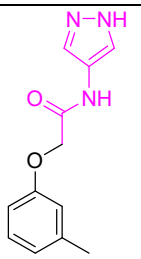	−6.7	**50**	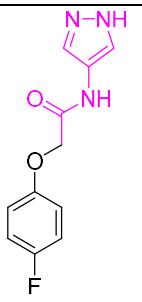	−8.3
51	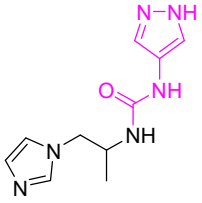	−7.6	**52**	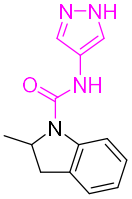	−8.3
53	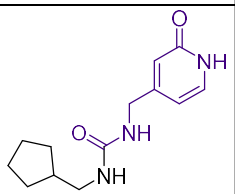	−8.4	**54**	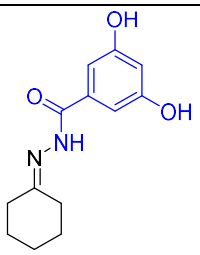	−6.9
55	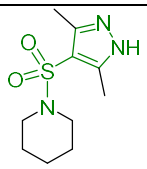	−7.8	**56**	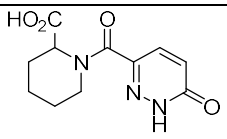	−6.7
57	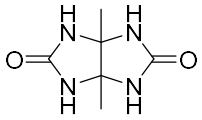	−6.5	**58**	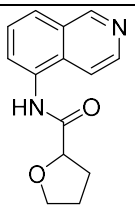	−6.8
59	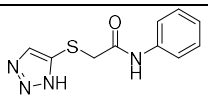	−7.5	**60**	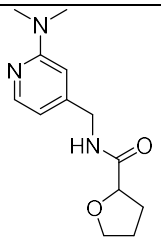	−6.9
61	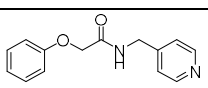	−6.4	**62**	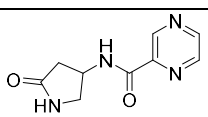	−6.6

63	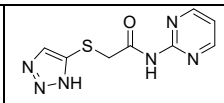	−6.9	**64**	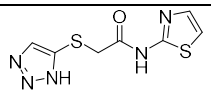	−6.7

[a]The scaffolds of the virtual hits that were selected for the design of the target hybrids are highlighted in colour.

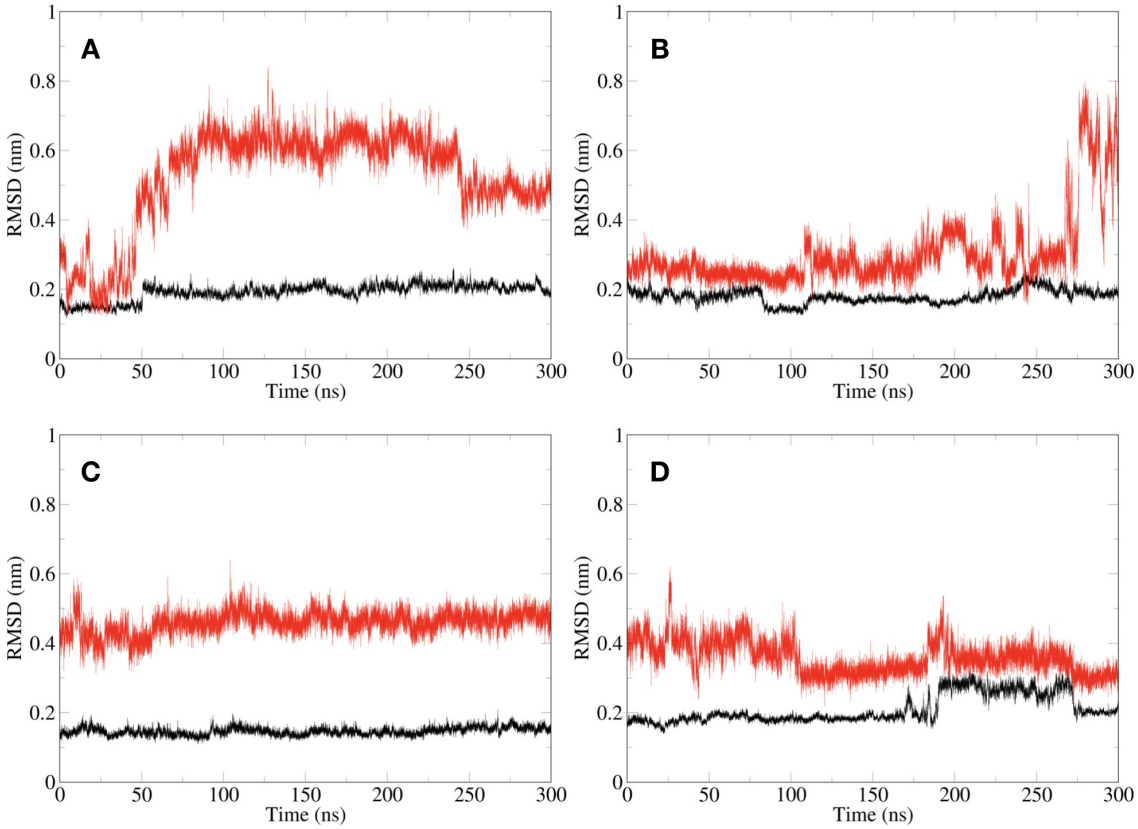

Fig. S2. RMSD analysis for protein backbone (black) and ligand (red) for the MD simulated complexes of BACE-1 with (7*R*,11*R*)-**11** (A), (7*R*,11*R*)-**10** (B), (7*S*,11*S*)-**11** (C) and (7*S*,11*S*)-**10**. The RMSD profiles were determined relative to the energy-minimized structure obtained after manual placement of compounds **11** and **10** along the groove guided by the arrangement of the rhein–huprine hybrid **1** and the pose of the VHS fragments.

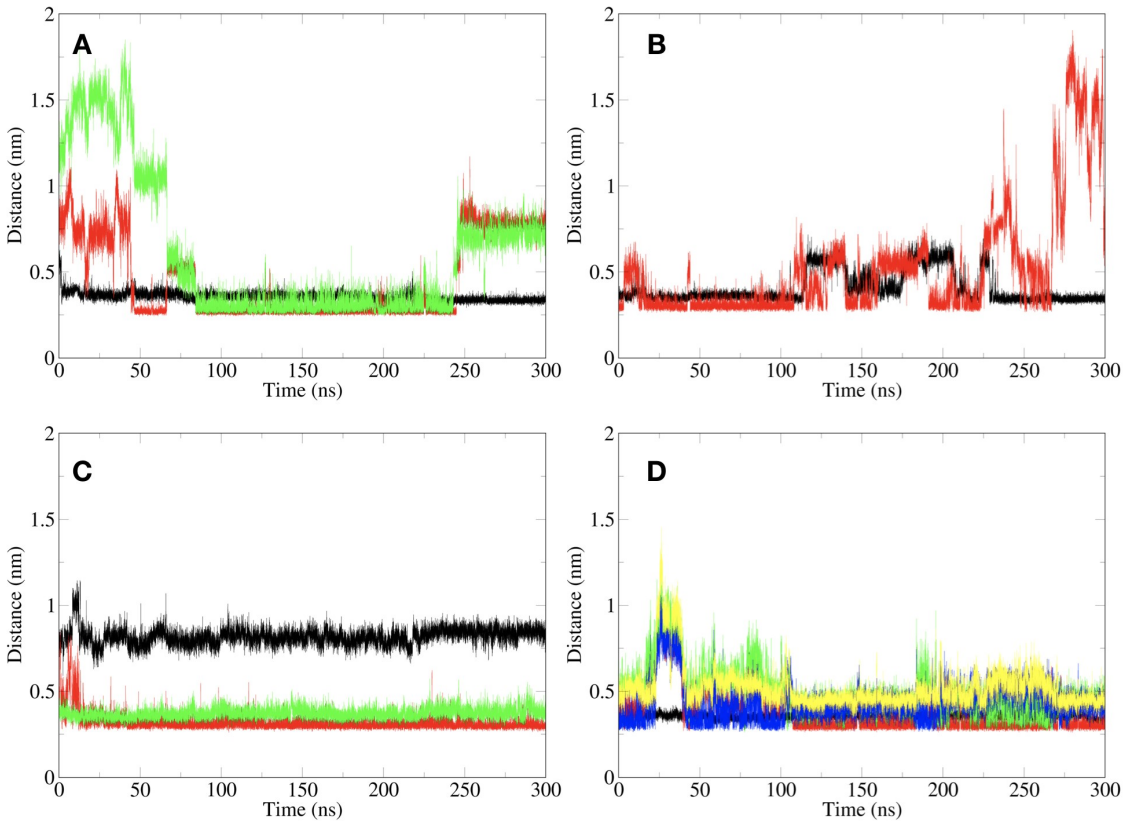

Fig. S3. Distance analysis for selected interactions between compounds **10** and **11** and residues in BACE-1 for (7*R*,11*R*)-**11** (A), (7*R*,11*R*)-**10** (B), (7*S*,11*S*)-**11** (C), and (7*S*,11*S*)-**10**. (A–D) black: The protonated quinoline nitrogen of the huprine moiety and the carbon atom of the carboxylic group of Asp32. (A) The hydroxyl groups of 3,5-dihydroxybenzamide of **11** and the backbone oxygens of (red) Phe322 and (green) Trp262. (B) red: The sulfonamide oxygen of **10** and the amide nitrogen of Asn233 (red). (C**)** red: The protonated quinoline nitrogen of the huprine moiety of **11** and the hydroxyl group of Thr72; green: The center-of-mass (COM) of the benzene moiety of **11** and the guanidinium group of Arg307. (D) red: The sulfonamide nitrogen of **10** and the carbonyl oxygen of Asn233; green/blue: The sulfonamide oxygens of **10** and the amide nitrogen of Asn233; yellow: The COM of the pyrazole ring of **10** and the Nε atom of Arg307.

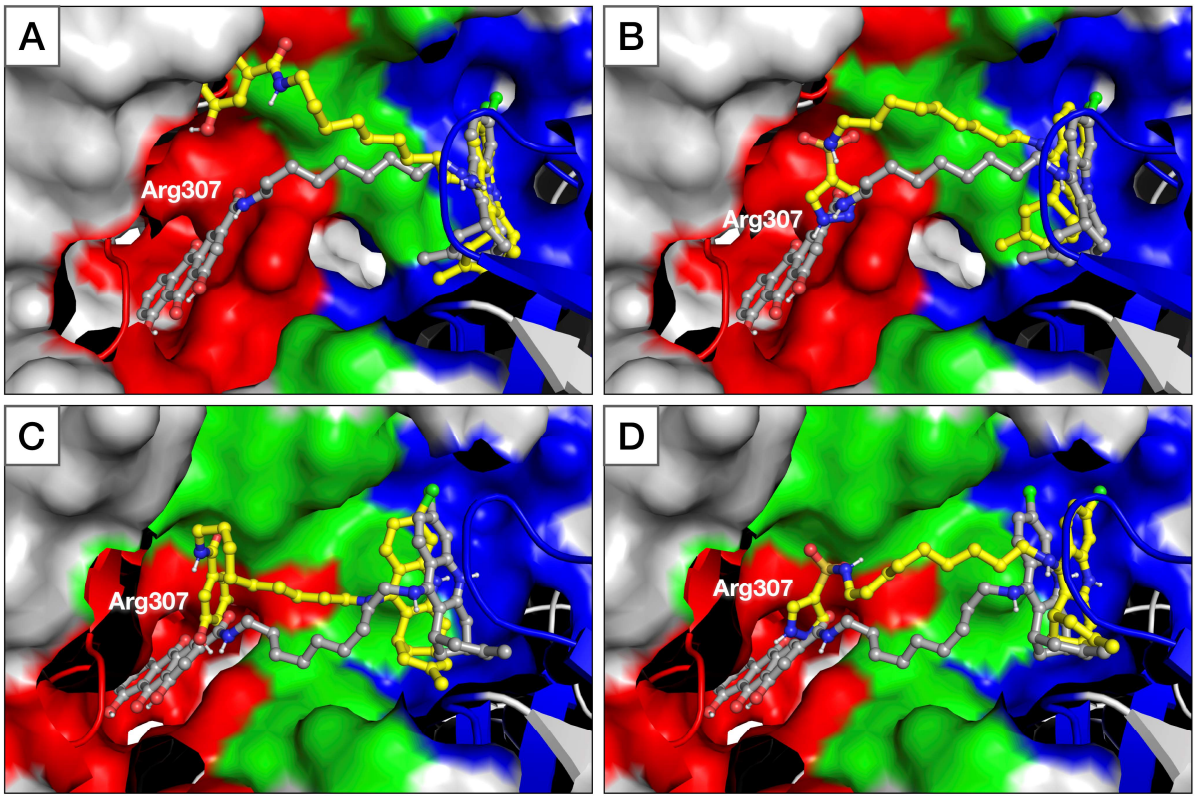

Fig. S4. Comparison of the simulated complexes of BACE-1 with (A) (7*R*,11*R*)-**11**, (B) (7*R*,11*R*)-**10**, (C) (7*S*,11*S*)-**11** and (D) (7*S*,11*S*)-**10** (ligand shown as yellow sticks) obtained at the end of the MD simulations with the binding mode found for the complex with the rhein–huprine hybrid **1** (shown as grey sticks). The catalytic site is highlighted in blue, the groove in green, and the secondary binding site in red onto the surface of a representative snapshot of the complex between BACE-1 and **1**.

***In vitro* determination of hBACE-1 inhibitory activity**

The inhibitory activity of the target compounds towards human recombinant BACE-1 (β-secretase, Invitrogen) was evaluated by employing the Panvera peptide as substrate. The substrate (10 μL, 250 nM final concentration) was added to 10 μL of solution of the target compounds or buffer in control wells (20 mM sodium acetate, pH 4.5, containing CHAPS 0.1% w/v). To start the reaction the enzyme was added (10 μL, 12.91 mU). The enzyme was left to react for 1 h at 37 ºC. The fluorescence signal was read at λ_{em} = 544 nm (λ_{ex} = 590 nm) after adding 10 μL of STOP solution (2.5 M sodium acetate). The DMSO concentration in the final mixture was maintained below 5% (v/v) to guarantee no significant loss of enzyme activity. The fluorescence intensities with and without inhibitor were compared and the percent of inhibition due to the presence of the target compounds was calculated. The background signal was measured in control wells containing all the reagents, except BACE-1, and was subtracted. The % of inhibition due to the presence of increasing concentrations of the test compounds was calculated by the following expression: $100 – (IF_i/IF_o \times 100)$, where IF_i and IF_o are the fluorescence intensities obtained for BACE-1 in the presence and in the absence of inhibitor, respectively. The IC_{50} values were extrapolated from the corresponding dose–response curves. Results are expressed as mean ± SEM of at least two experiments, each performed in triplicate. Data analysis was performed with GraphPad Prism 4.03 software (GraphPad Software Inc.).

In vitro determination of hAChE and hBChE inhibitory activity

The *in vitro* inhibitory activity of the target compounds towards human recombinant AChE and human serum BChE (Sigma, Milan, Italy) was evaluated spectrophotometrically. The enzyme stock solutions were prepared by dissolving enzyme-lyophilized powders in 0.1% Triton X-100/0.1 M potassium phosphate, pH 8.0 (for hAChE inhibition assay) or in 0.1% aq. gelatin (for the hBChE inhibition assay). The stock solutions of the target compounds (1 mM) were prepared in MeOH. The assay solution consisted of 340 μM 5,5'-dithiobis(2-nitrobenzoic acid) (DTNB), 0.02 unit/mL hAChE or hBChE, and 550 μM substrate (acetylthiocholine iodide or butyrylthiocholine iodide, for AChE and BChE inhibition assays, respectively), in 0.1 M potassium phosphate, pH 8.0. Assay solutions with and without the target compounds were preincubated at 37 °C for 20 min, before the addition of the substrate. Blank solutions containing all components except the enzymes were prepared in parallel to correct for the non-enzymatic hydrolysis of the substrates. Initial rates were monitored at 412 nm with a Jasco V-530 double beam spectrophotometer equipped with thermostated cuvette holders (37 °C). At least five increasing concentrations of the target compounds, which led to 20–80% inhibition of the enzymatic activities, were assayed. IC_{50} values were calculated using Microcal Origin 3.5 software (Microcal Software, Inc), and are expressed as mean ± SEM of at least two experiments, each performed in triplicate.

Determination of the Aβ42 and tau antiaggregating activity in intact *E. coli* cells

E. coli BL21 (DE3) competent cells were transformed with the pET28a vector (Novagen, Inc., Madison, WI, USA), which carries the DNA sequence of Aβ42, or with pTARA, which contains the RNA-polymerase gen of T7 phage (T7RP) under the control of the promoter PBAD, and were then transformed with the pRKT42 vector, encoding four repeats of tau protein in two inserts. M9 minimal medium (10 mL) containing kanamycin (50 μg/mL) (for Aβ42 overexpression) or glucose (0.5%), ampicillin (50 μg/mL) and chloramphenicol (12.5 μg/mL) (for tau overexpression) were inoculated with a colony of BL21 (DE3) cells bearing the plasmids. The volume of overnight culture necessary to get a 1:500 dilution was added to fresh M9 minimal medium containing kanamycin (50 μg/mL) and thioflavin-S (Th-S, 250 μM) (for Aβ42 overexpression) or glucose (0.5%), ampicillin (50 μg/mL), chloramphenicol (12.5 μg/mL), and Th-S (250 μM) (for tau overexpression). The cultures were grown at 37 ºC and 250 rpm overnight until cell density reached OD_{600} = 0.6. An aliquot part of the cultures (980 μL) was transferred into 1.5 mL Eppendorf tubes that contained a solution of the target compound in DMSO (10 μL) and isopropyl 1-thio-β-D-galactopyranoside (IPTG, 10 μL at 100 mM) (for Aβ42 overexpression) or arabinose (10 μL at 25%) (for tau overexpression), leading to a final inhibitor concentration of 10 μM. The resulting cultures were grown at 37 °C and 1400 rpm overnight with a Thermomixer (Eppendorf, Hamburg, Germany). The same amount of DMSO without the target compound was added to the sample as a negative control (maximal amount of Aβ42 or tau), whereas non-induced samples (in the absence of IPTG or arabinose) were prepared as positive controls (absence of Aβ42 or tau), and to assess the potential intrinsic toxicity of the target compounds.

The Aβ42 and tau anti-aggregating activity of the target compounds was assessed using a fluorescence assay, by employing a 2500 mM stock solution of Th-S (T1892, Sigma, St. Louis, MO, USA) in double-distilled water (Milli-Q system, Millipore, USA). The Th-S spectra were measured on an Aminco Bowman Series 2 luminescence spectrophotometer (Aminco-Bowman AB2, SLM Aminco, Rochester, NY, USA) in the range 460–600 nm at 25 °C, with an excitation wavelength of 440 nm and slit widths of 4 nm, and an emission wavelength of 485 nm. The results are the average of nine independent experiments, each performed in triplicate. As positive controls we used the known Aβ42 antiaggregating agent propidium iodide and DP128, a known Aβ42 and tau antiaggregating compound.

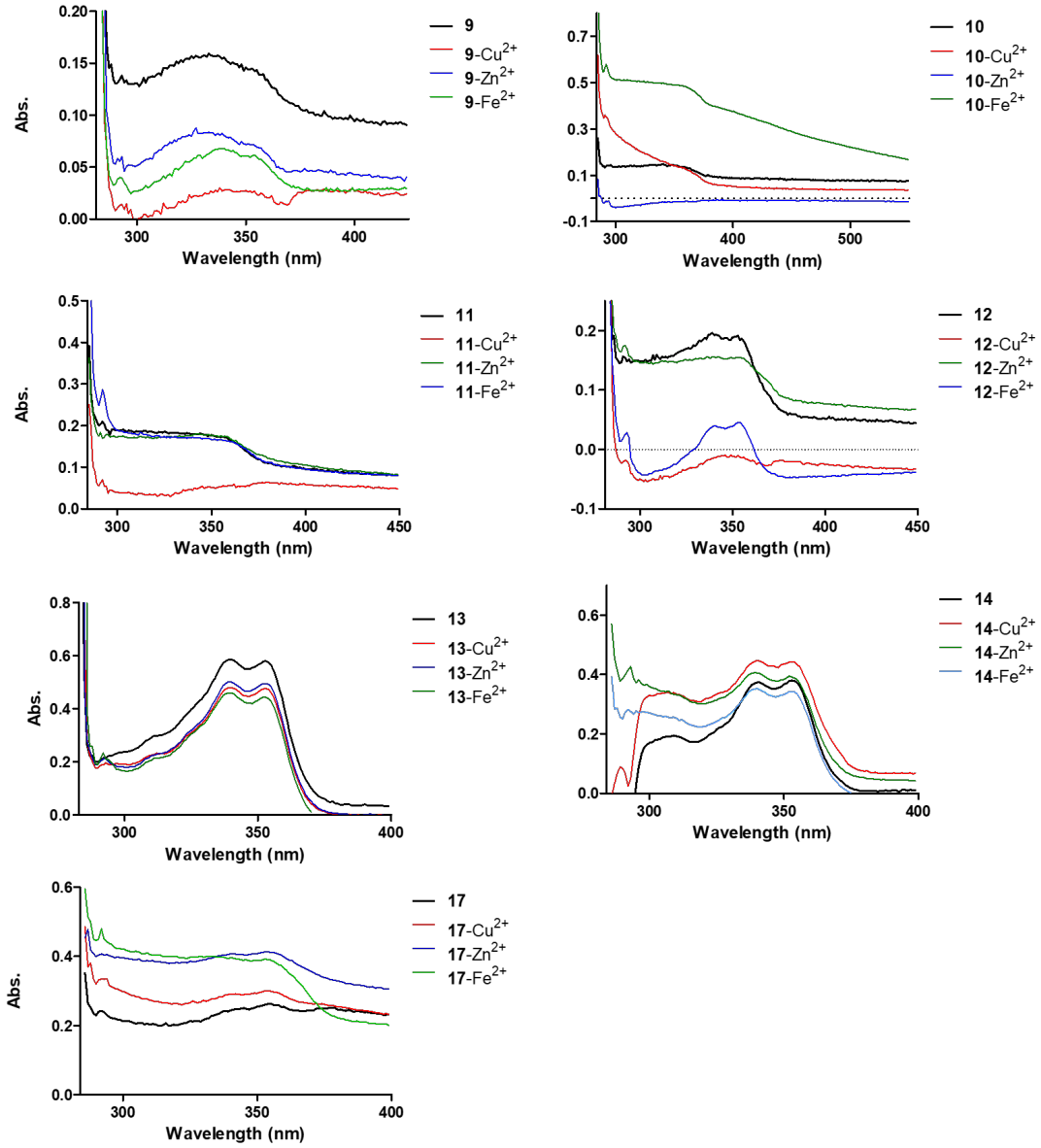

Fig. S5. UV/vis absorption spectra of compounds **9**–**14** and **17** (60 μM in 20 mM HEPES buffer pH = 7.4, 150 mM NaCl) in the absence and presence of metal salts (60 μM).

Table S3

Percent Cu^{2+} chelation ability and antioxidant activity of target and reference compounds

Compd	Compound:Cu^{2+} ratio[a]				DPPH[b]
	5:1	2:1	1:1	0.5:1	EC_{50} (μM) (or % scavenging @500 μM)
9	75.2 ± 2.7	42.9 ± 4.9	22.2 ± 2.6	16.8 ± 4.5	(55.5 ± 11.4)
10	100 ± 1	97.4 ± 1.4	93.5 ± 2.5	86.7 ± 6.6	(70.8 ± 10.2)
11	29.2 ± 2.8	14.5 ± 5.1	13.9 ± 7.1	11.4 ± 5.4	(39.4 ± 9.4)
12	96.4 ± 1.9	92.6 ± 2.9	88.1 ± 4.1	80.2 ± 6.4	19.6 ± 1.1
13	63.2 ± 10.8	42.2 ± 10.1	20.9 ± 6.1	20.4 ± 5.4	na[c]
14	41.4 ± 4.5	21.7 ± 2.5	15.3 ± 8.1	17.1 ± 8.4	90.6 ± 4.0
17	35.0 ± 5.5	17.4 ± 5.3	18.4 ± 5.7	20.1 ± 9.8	na[c]
EDTA	102 ± 0	101 ± 0	100 ± 1	59.9 ± 7.3	
Ascorbic acid					11.8 ± 0.5

[a]Cu^{2+} chelation ability is expressed as mean % ± SD of three independent experiments, each performed in duplicate. [b]% DPPH radical scavenging activity at 500 μM or EC_{50} (μM). Values are expressed as mean ± SD of three independent experiments, each performed in duplicate. [c]na: not active.

Neuroprotection and neurotoxicity assay in HT22 cells

HT22 mouse hippocampal neuronal cells were grown in Dulbecco's modified Eagel's medium (DMEM, Sigma-Aldrich, Darmstadt, Germany) supplemented with 10% (v/v) heat-inactivated fetal calf serum (FCS) containing 1% penicillin/streptomycin. Cells were passaged every 2 days and incubated at 37 °C with 5% CO_2 in a humidified incubator. Stock solutions of the target compounds were prepared in DMSO (Sigma-Aldrich, Darmstadt, Germany) and diluted with medium. Generally, 80% confluent cells were seeded with 5000 cells per well (in 100 µL) into sterile 96-well plates and incubated for 24 h. For the neurotoxicity assay, the previous medium in each well was replaced by 100 µL of different compound dilutions, prepared in growth medium. DMSO (0.83%) in growth medium served as control. Cells were incubated for 24 h with the target compounds. After incubation, cell viability was determined using the 3-(4,5-dimethylthiazol-2-yl)-2,5-diphenyl tetrazolium bromide (MTT, Sigma-Aldrich, Darmstadt, Germany) assay. For the neuroprotection assay, the previous medium in each well was replaced by different compound dilutions, prepared in growth medium containing 5 mM glutamate. After incubation for 24 h, cell viability was determined using the MTT assay. Treatment with quercetin (25 µM) served as positive control for neuroprotection. For the assessment of cell viability, MTT-solution (4 mg/mL in PBS) was diluted 1:10 with growth medium and 100 µL were added to each well after careful removal of previous medium containing the compound. After incubation for 3 h the supernatant was carefully removed and 100 µL lysis buffer (10% SDS in double-distilled H_2O) was applied. The following day, absorbance at 560 nm was determined using a multiwell plate photometer (Tecan, SpectraMax 250). Results are presented as percentage to untreated control cells. Data are expressed as mean ± SD of three independent experiments, each performed in sextuplicate. Analysis was performed using GraphPad Prism 5 software, applying one-way ANOVA followed by Bonferroni multiple comparison post-test. Levels of significance: $*p < 0.05$; $**p < 0.01$; $***p < 0.001$; $\#p < 0.05$; $\#\#p < 0.01$ $\#\#\#p < 0.001$.

Table S4

Neuroprotective effects of compounds 9–12 against glutamate-induced oxidative stress in neuronal HT22 cells

	Cell viability (% of control)[a]			
Compd	1 μM	5 μM	10 μM	25 μM
Glu 5 mM	10.3 ± 1.5			
Glu 5 mM + **9**	13.6 ± 3.1	10.1 ± 1.8	10.0 ± 2.8	20.5 ± 6.9
Glu 5 mM + **10**	12.2 ± 2.1	15.1 ± 7.5	13.9 ± 7.5	7.0 ± 1.8
Glu 5 mM + **11**	12.5 ± 2.3	12.9 ± 5.0	10.0 ± 4.1	10.5 ± 4.4
Glu 5 mM + **12**	12.9 ± 2.9	12.6 ± 1.7	19.9 ± 6.5	62.2 ± 11.3
Glu 5 mM + quercetin				62.6 ± 6.6

[a]Viability of neuronal HT22 cells treated with 5 mM glutamate (Glu) alone or in combination with different concentrations of the target compounds (1, 5, 10, or 25 μM) or quercetin (25 μM). Results are presented as means ± SD of three independent experiments, each performed in sextuplicate, and refer to untreated control cells, which were set as 100% values.

Table S5

Neurotoxicity of the target hybrids on neuronal HT22 cells

	Cell viability (% of control)[a]			
Compd	1 μM	5 μM	10 μM	25 μM
9				94.8 ± 16.2
10	103.0 ± 15.8	95.1 ± 10.0	81.1 ± 11.7	80.5 ± 12.9
11				103.8 ± 10.3
12	91.7 ± 12.2	90.4 ± 10.1	98.6 ± 11.1	90.7 ± 14.9
13				101.2 ± 15.2
14	109.5 ± 11.5	106.8 ± 12.2	105.2 ± 11.6	102.5 ± 15.0
17				100.2 ± 14.7

[a]Viability of HT22 cells treated with different concentrations (1, 5, 10, and 25 μM) of **10**, **12**, and **14** or 25 μM of **9**, **11**, **13**, and **17**. Results are presented as means ± SD of three independent experiments, each performed in sextuplicate, and refer to untreated control cells, which were set as 100% values.

In vitro brain permeability: PAMPA-BBB assay

The compounds were dissolved in PBS/EtOH 70:30 and their permeabilities were determined through a lipid extract of porcine brain membrane. The assay was validated by comparison of the experimental and reported P_e values of a set of fourteen commercial drugs (Supplementary Table S4). The following correlation was obtained: P_e (exp) = 1.6436 P_e (lit) – 1.3599 (R^2 = 0.9360). Considering this equation and the limits established by Di *et al.* for BBB permeation, the threshold for high BBB permeation (CNS+) was set at P_e (10^{-6} cm/s) > 5.21; whereas the range for low BBB permeation (CNS–) was set at P_e (10^{-6} cm/s) < 1.93, and that for uncertain BBB permeation (CNS±) at 5.21 > P_e (10^{-6} cm/s) > 1.93. Data are expressed as the mean ± SD of three independent experiments, each performed in triplicate.

Table S6

Reported and experimental permeability (*Pe* 10^{-6} cm s^{-1}) Values in the PAMPA-BBB assay of 14 commercial drugs used for assay validation.

Compound	Bibliography value[a]	Experimental value (n = 3) ± S.D.
Cimetidine	0.0	0.7 ± 0.1
Lomefloxacin	1.1	0.9 ± 0.1
Norfloxacin	0.1	0.9 ± 0.1
Ofloxacin	0.8	1.0 ± 0.1
Hydrocortisone	1.9	1.4 ± 0.1
Piroxicam	2.5	2.2 ± 0.1
Clonidine	5.3	6.5 ± 0.1
Corticosterone	5.1	6.7 ± 0.1
Imipramine	13.0	12.3 ± 0.1
Promazine	8.8	13.8 ± 0.3
Progesterone	9.3	16.8 ± 0.3
Desipramine	12.0	17.8 ± 0.1
Testosterone	17.0	27.2 ± 0.4
Verapamil	16.0	28.3 ± 0.5

[a]Taken from Di, L.; Kerns, E. H.; Fan, K.; McConnell, O. J.; Carter, G. T. High throughput artificial membrane permeability assay for blood-brain barrier. *Eur. J. Med. Chem.* **2003**, *38*, 223–232.

Molecular analysis. Western blotting

The hippocampus tissue from each animal was homogenized in lysis buffer (Tris HCl pH 7.4, NaCl 150 mM, EDTA 5 mM and 1X-Triton X-100) that contained phosphatase and protease inhibitors (Cocktail II, Sigma-Aldrich, St. Louis, MO) to obtain total protein homogenates. The Bradford technique was used to determine total protein concentration. Aliquots of 15 µg of total hippocampal protein were separated by sodium dodecyl sulfate-polyacrylamide gel electrophoresis (SDS-PAGE) (8–20%) and transferred into polyvinylidene difluoride (PVDF) membranes (Millipore, Burlington, MA, USA) for 2 h. The membranes were then blocked in 5% non-fat milk in TRIS-buffered saline (TBS) containing 0.1% Tween 20 (TBS-T, Sigma-Aldrich) for 1 h at rt, and then, overnight incubation was carried out at 4 ºC with the primary antibodies listed in Supplementary Table S5. The membranes were washed with TBS-T 3 times for 5 min and incubated with secondary antibodies for 1 h at rt. Immunoreactive protein was viewed with a Chemiluminescence-based detection kit, following the manufacturer's protocol (ECL Kit; Millipore), and digital images were acquired using a ChemiDoc XRS+ System (BioRad lab, Hercules, CA, USA). Semi-quantitative analyses were done using ImageLab Software (BioRad Lab), and results were expressed in Arbitrary Units (AU) considering control protein levels as 100%. Protein loading was routinely monitored by immunodetection of glyceraldehyde-3-phosphate dehydrogenase (GADPH).

Table S7

Antibodies used in Western Blot (WB) and immunohistochemistry studies.

Antibody	Host	Source/Catalog/RRID	WB dilution
pGSK3β (Ser 9)	Rabbit	Cell Signaling/#9322S/D3A4	1:1000
GSK3β Total	Rabbit	Cell Signaling/#12456S/D5C5Z)	1:1000
PSD95	Rabbit	Abcam/ab18258/AB_444362	1:1000
p-Tau (Ser404)	Rabbit	Invitrogen/44758G/AB_2533746	1:1000
sAPPα	Rabbit	Covance/SIG39139/ AB_10721469	1:500
sAPPβ	Rabbit	Covance/SIG-39138-050/ AB_66287	1:500
SYN	Mouse	Millipore/MAB5258/ AB_2313839	1:1000
Tau Total	Mouse	Invitrogen/AHB0042/AB_2533746	1:1000
GAPDH	Mouse	Millipore/MAB374/ AB_2107445	1:2500
Goat-anti-mouse HRP conjugated		Biorad Lab/170-5047/AB_11125753	1:6000
Goat-anti-rabbit HRP conjugated		Biorad Lab/170-6515/AB_11125142	1:6000

RNA extraction and determination of gene expression by q-PCR

Total RNA isolation from hippocampal tissue was carried out using TRIsure™ reagent following the manufacturer's instructions (Bioline Reagents, London, UK). The yield, purity, and quality of RNA were determined spectrophotometrically with a NanoDrop™ ND-1000 (ThermoFisher Scientific, Waltham, MA, USA) apparatus and an Agilent 2100B Bioanalyzer (Agilent Technologies, Santa Clara, CA, USA). RNAs with 260/280 ratios and RIN higher than 7.5, respectively, were selected. Reverse transcription-polymerase chain reaction (RT-PCR) was performed as follows: 2 μg of messenger RNA (mRNA) was reverse-transcribed using the High-capacity cDNA reverse transcription Kit (Applied Biosystems, Foster City, CA, USA). Real-time quantitative PCR (qPCR) was used to quantify mRNA expression genes listed in Supplementary Table S6.

Real-time PCR was performed by using Step One Plus Detection System (Applied-Biosystems) employing SYBR® Green PCR Master Mix (Applied-Biosystems). Each reaction mixture contained 6.75 μL of complementary DNA (cDNA) (2 μg/μL), 0.75 μL of each primer (100 nM), and 6.75 μL of SYBR® Green PCR Master Mix (2X) (Applied Biosystems).

Data were analyzed utilizing the comparative cycle threshold (Ct) method (ΔΔCt), where the housekeeping gene level was used to normalize differences in sample loading and preparation. Normalization of expression levels was performed with β-actin for SYBR® Green-based real-time PCR results. Each sample was analyzed in duplicate, and the results represent the n-fold difference of the transcript levels among different groups.

Table S8

Primers and probes used in qPCR studies.

Target	Product size (bp)	Forward primer (5'-3')	Reverse primer (5'-3')
Ide	287	CCAAAAGGAAGCGTTCGCC	GGGATCGCTGATGAGAAGCA
Nep	196	TTGGGAGACCTGGCGGAAAC	CATTCCTTGGACCCTCACCCC
Adam10	125	GGGAAGAAATGCAAGCTGAA	CTGTACAGCAGGGTCCTTGAC
Bace1	188	AAGCTGCCGTCAAGTCCATC	GCGGAAGGACTGATTGGTGA
Il-1β	179	ACAGAATATCAACCAACAAGTGATATTCTC	GATTCTTTCCTTTGAGGCCCA
Tnf-α	151	GTTTACAAGCATCCAGGCACAG	GAAGGTTTGAGGCGGCTTTC
Il-6	189	ATCCAGTTGCCTTCTTGGGACTGA	TAAGCCTCCGACTTGTGAAGTGGT
Cxcl10	72	GGCTAGTCCTAATTGCCCTTGG	TGTCTCAGGACCATGGCTTG
Ifn-γ	110	CCTTCTTCAGCAACAGCAAGGCG	CTTGGCGCTGGACCTGTGGG
Hmox1	177	TGACACCTGAGGTCAAGCAC	GTCTCTGCAGGGGCAGTATC
Cox-2	126	TGACCCCCAAGGCTCAAATA	CCCAGGTCCTCGCTTATGATC
Actin	190	CAACGAGCGGTTCCGAT	GCCACAGGTTCCATACCCA

Copies of ^{1}H NMR (400 MHz, CD_3OD) and ^{13}C NMR (100.6 MHz, CD_3OD) spectra and HPLC chromatograms of target compounds

N-{9-[(3-Chloro-6,7,10,11-tetrahydro-9-methyl-7,11-methanocycloocta[*b*]quinolin-12-yl)amino]nonyl}-2-hydroxypyridine-3-carboxamide (**9**)

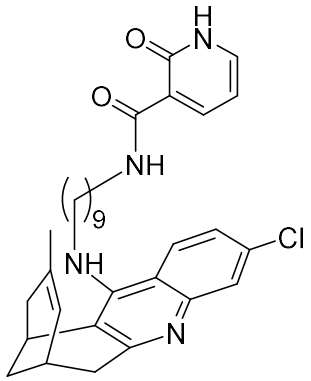

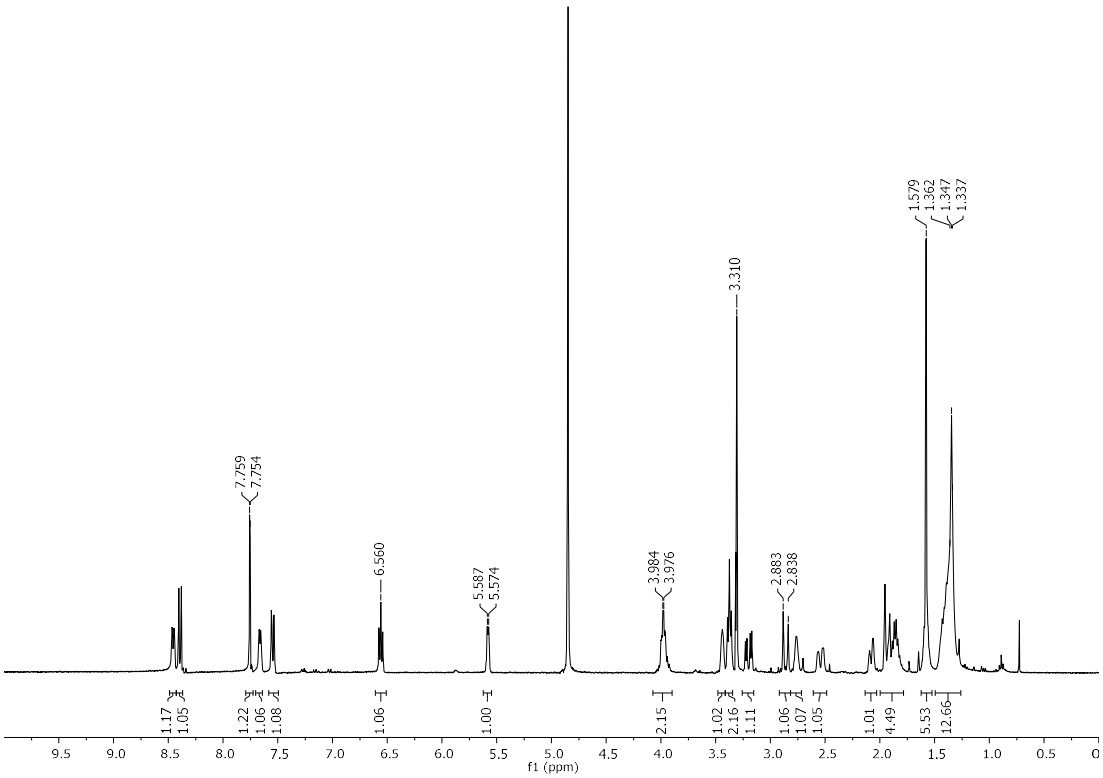

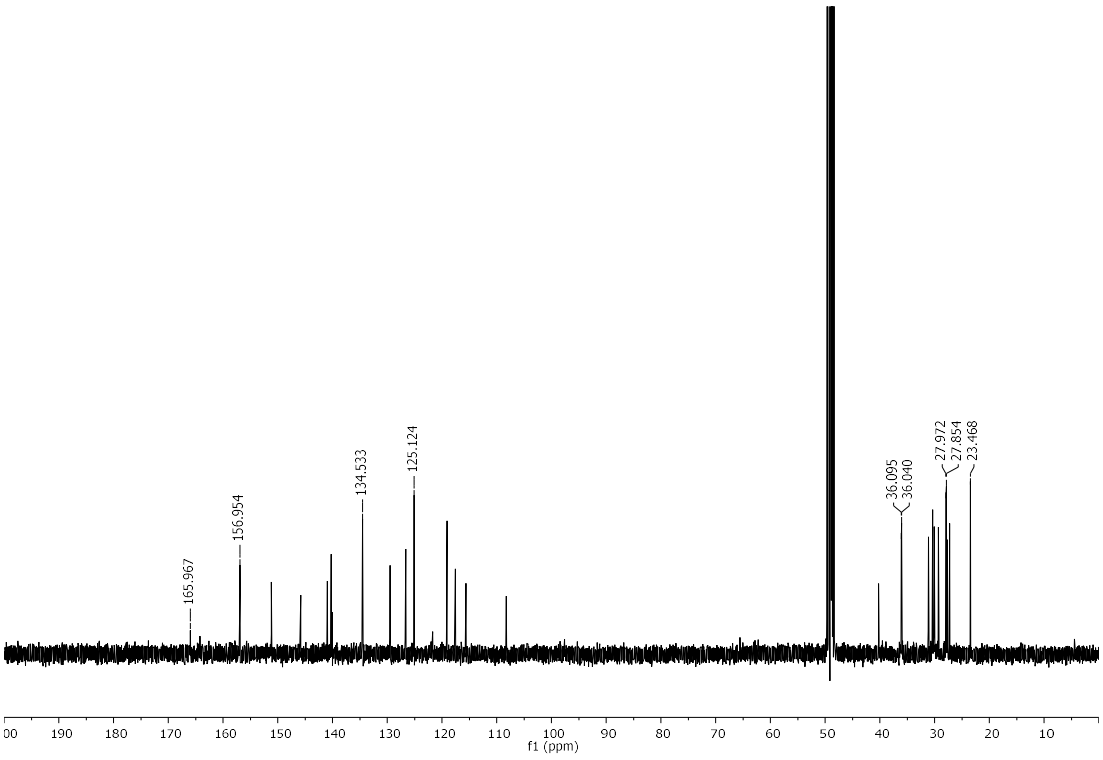
165.967
156.954
134.533
125.124
36.095
36.040
27.972
27.854
23.468
f1 (ppm)

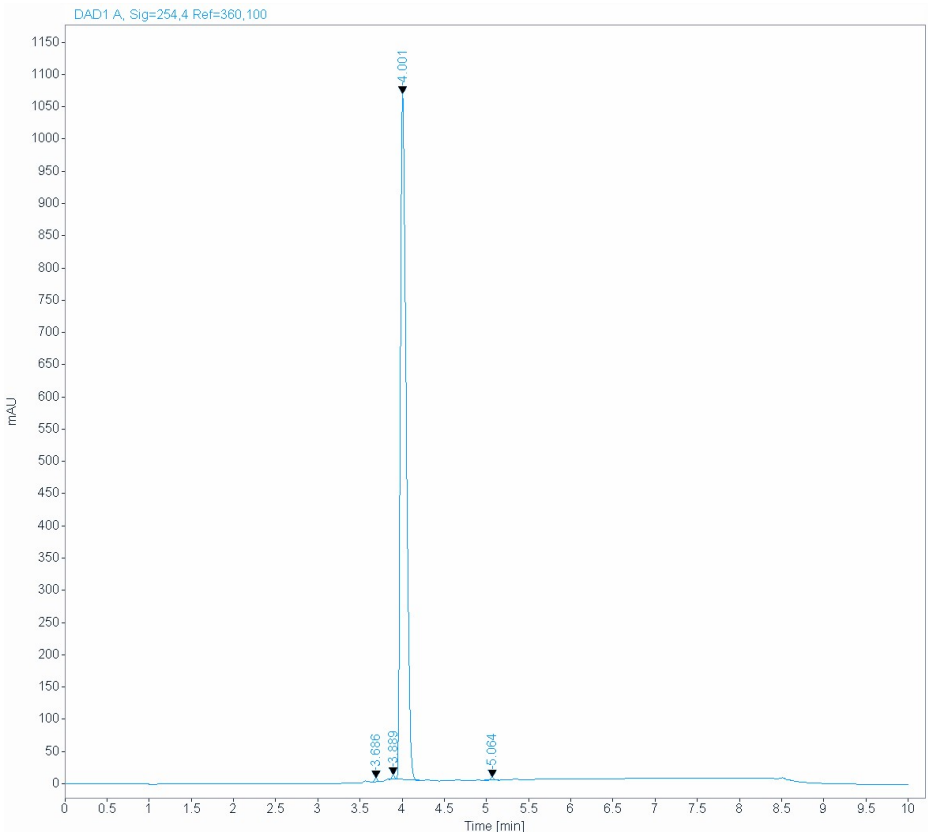
DAD1 A, Sig=254,4 Ref=360,100
mAU
Time [min]
4.001
3.686
3.889
5.064

N-{9-[(3-Chloro-6,7,10,11-tetrahydro-9-methyl-7,11-methanocycloocta[*b*]quinolin-12-yl)amino]nonyl}-1*H*-pyrazole-4-sulfonamide (**10**)

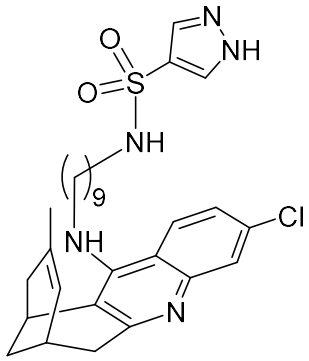

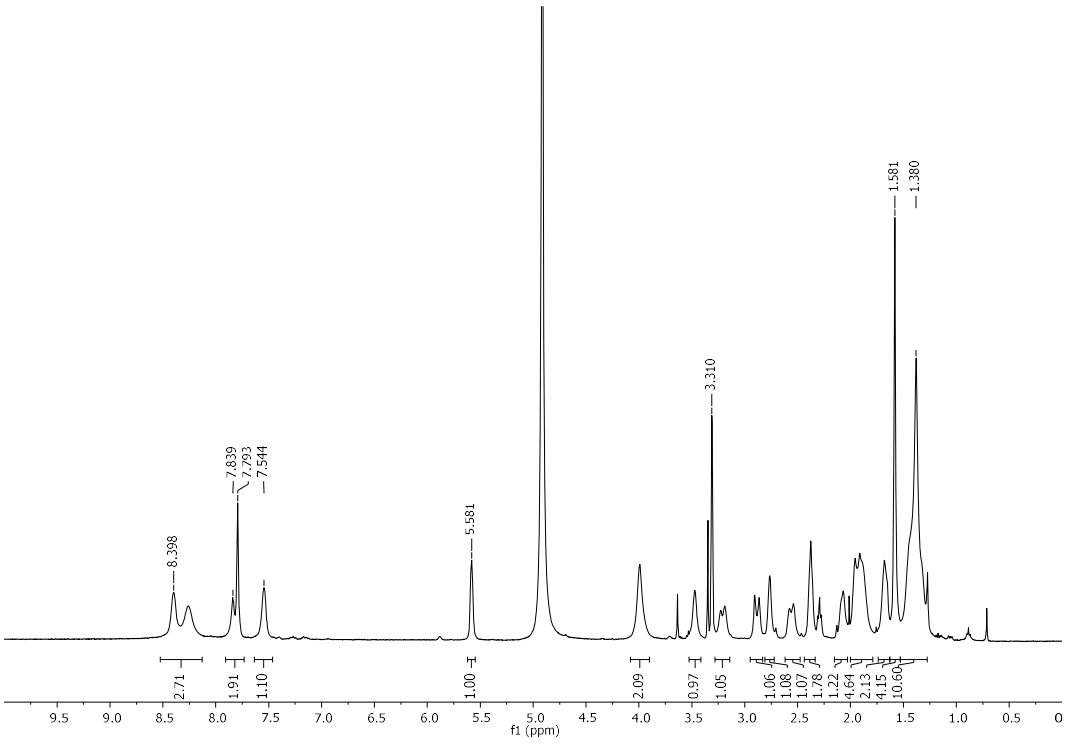

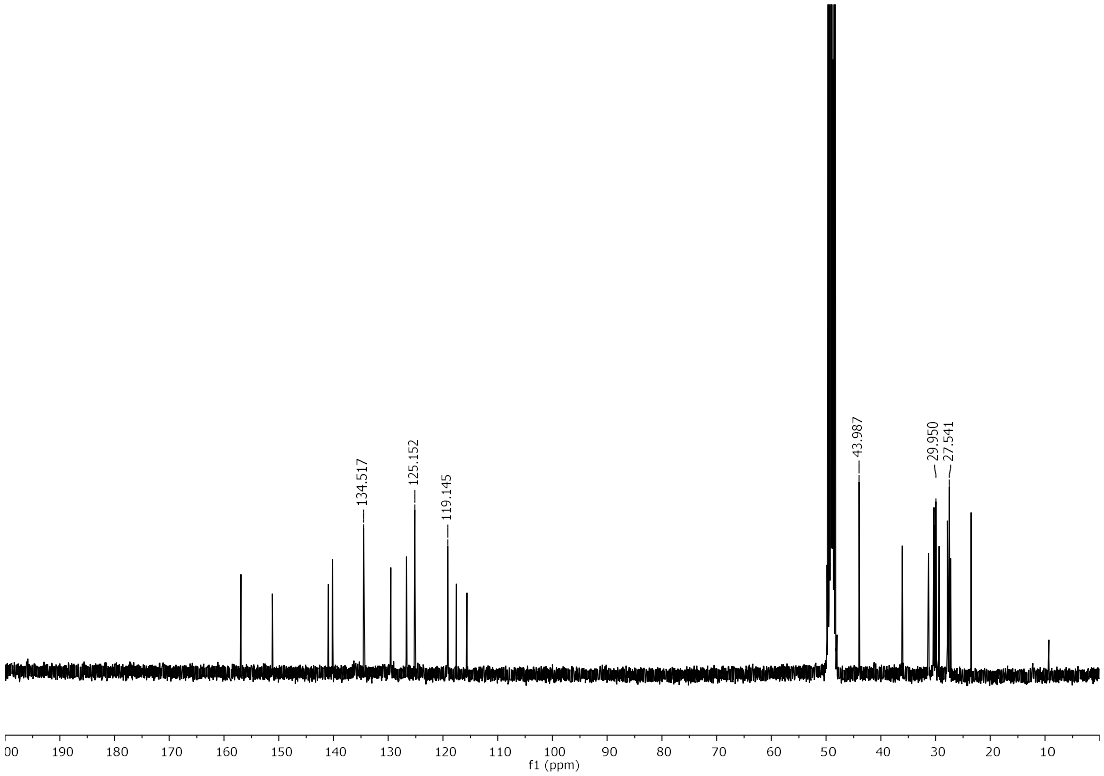
134.517
125.152
119.145
43.987
29.950
27.541
f1 (ppm)

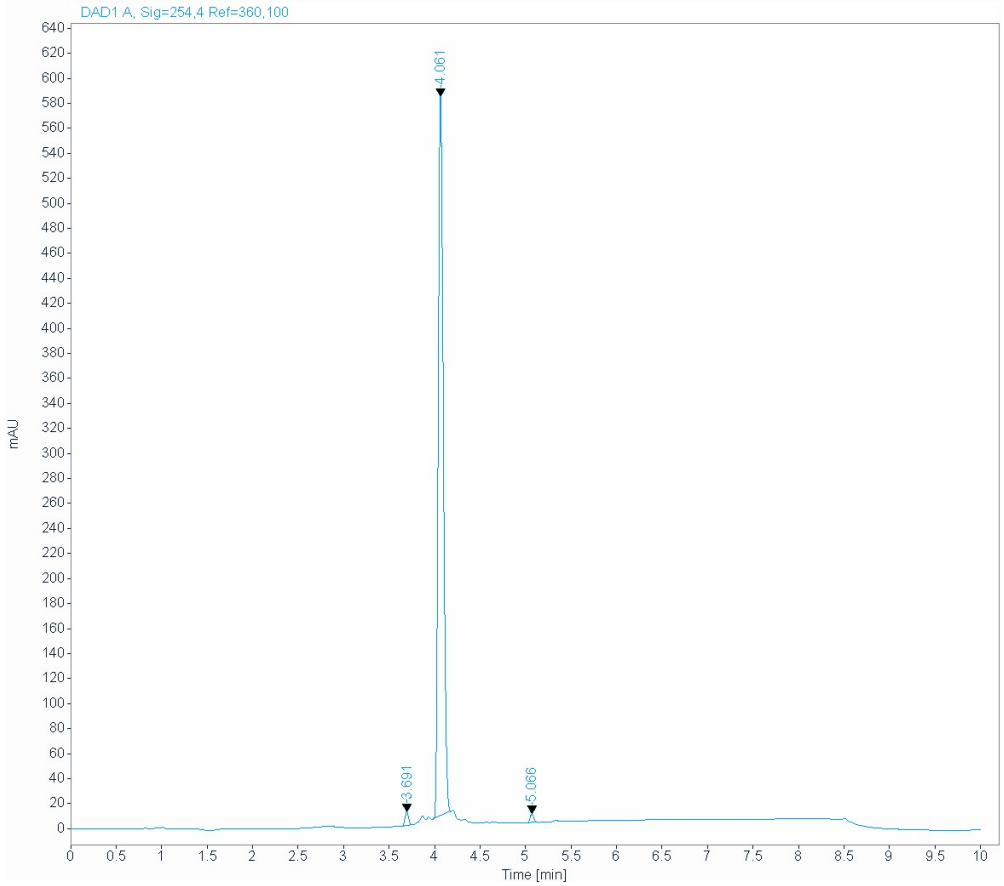
DAD1 A, Sig=254,4 Ref=360,100
mAU
Time [min]
4.061
3.691
5.066

N-{9-[(3-Chloro-6,7,10,11-tetrahydro-9-methyl-7,11-methanocycloocta[*b*]quinolin-12-yl)amino]nonyl}-3,5-hydroxybenzamide (**11**)

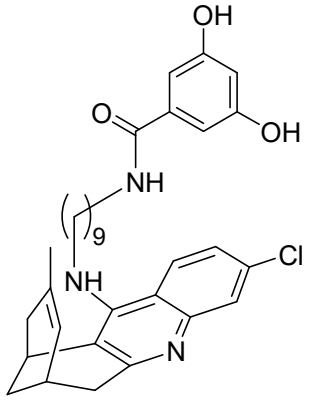

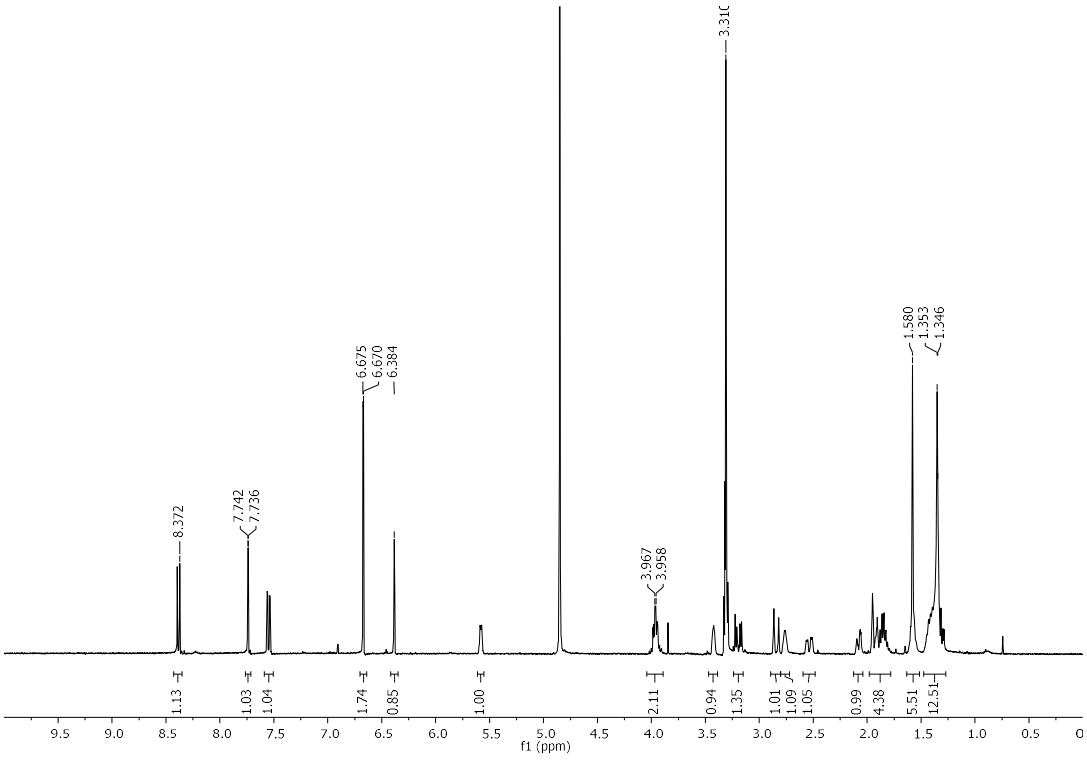

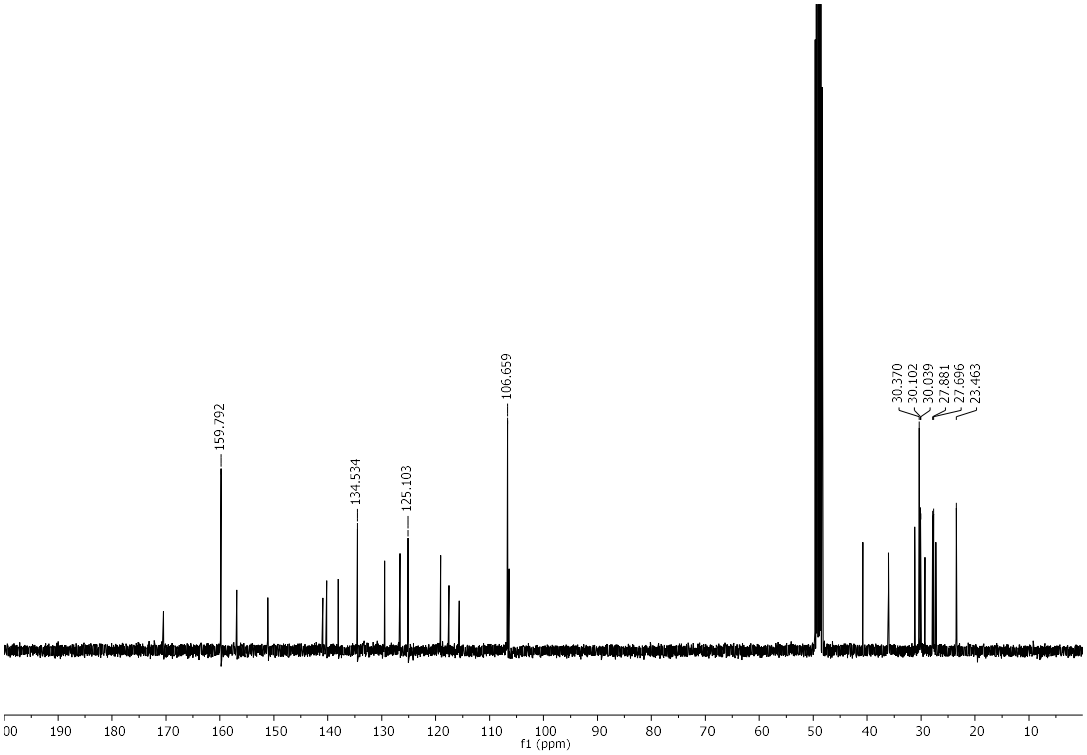
159.792
134.534
125.103
106.659
30.370
30.102
30.039
27.881
27.696
23.463
f1 (ppm)

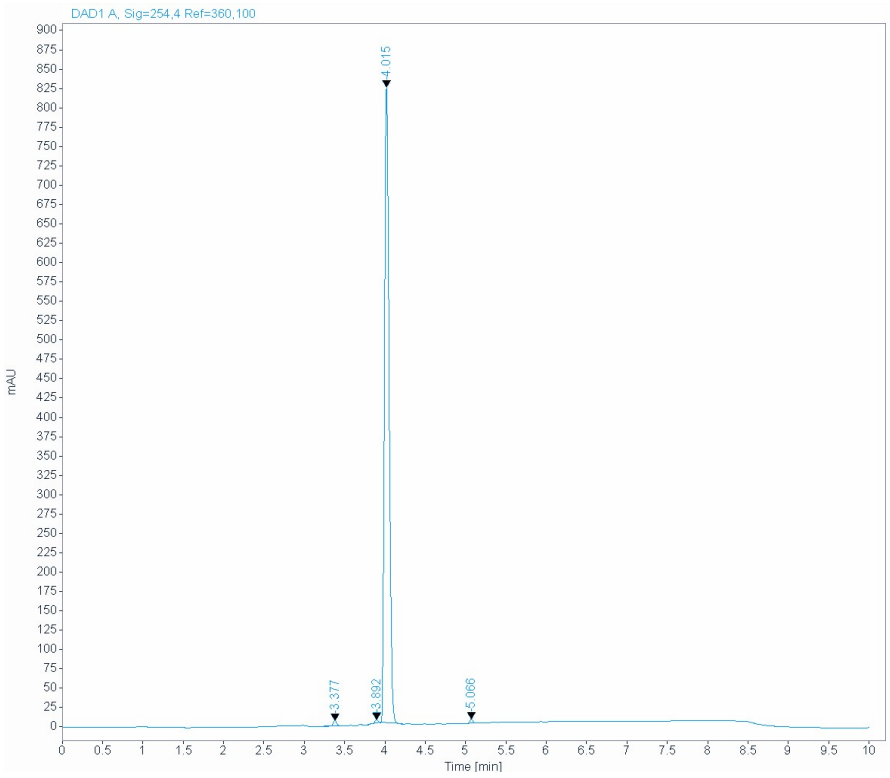
DAD1 A, Sig=254,4 Ref=360,100
mAU
Time [min]
4.015
3.377
3.892
5.066

9-[(3-Chloro-6,7,10,11-tetrahydro-9-methyl-7,11-methanocycloocta[*b*]quinolin-12-yl)amino]-*N*-(1*H*-pyrazol-4-yl)nonanamide (**12**)

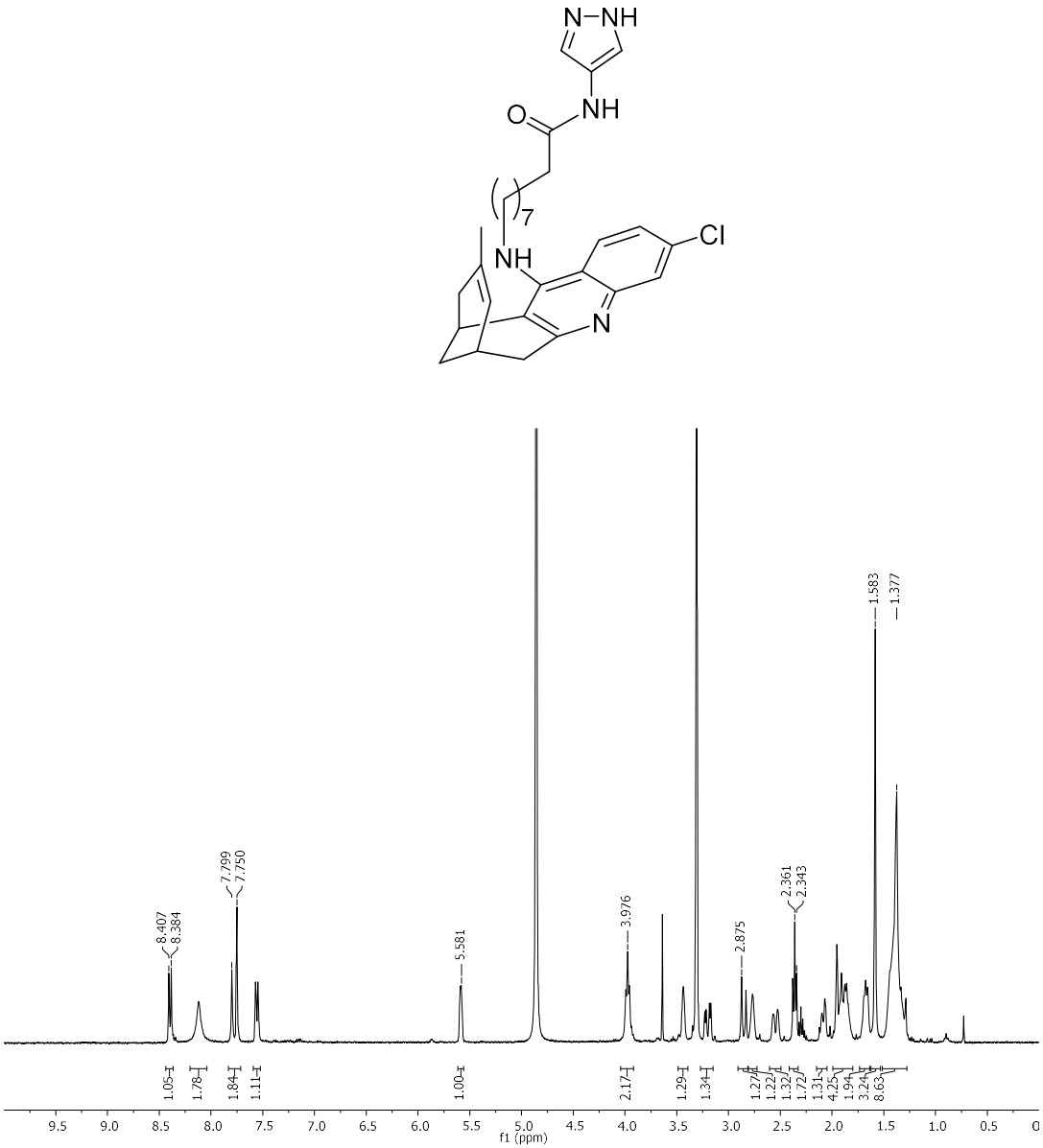

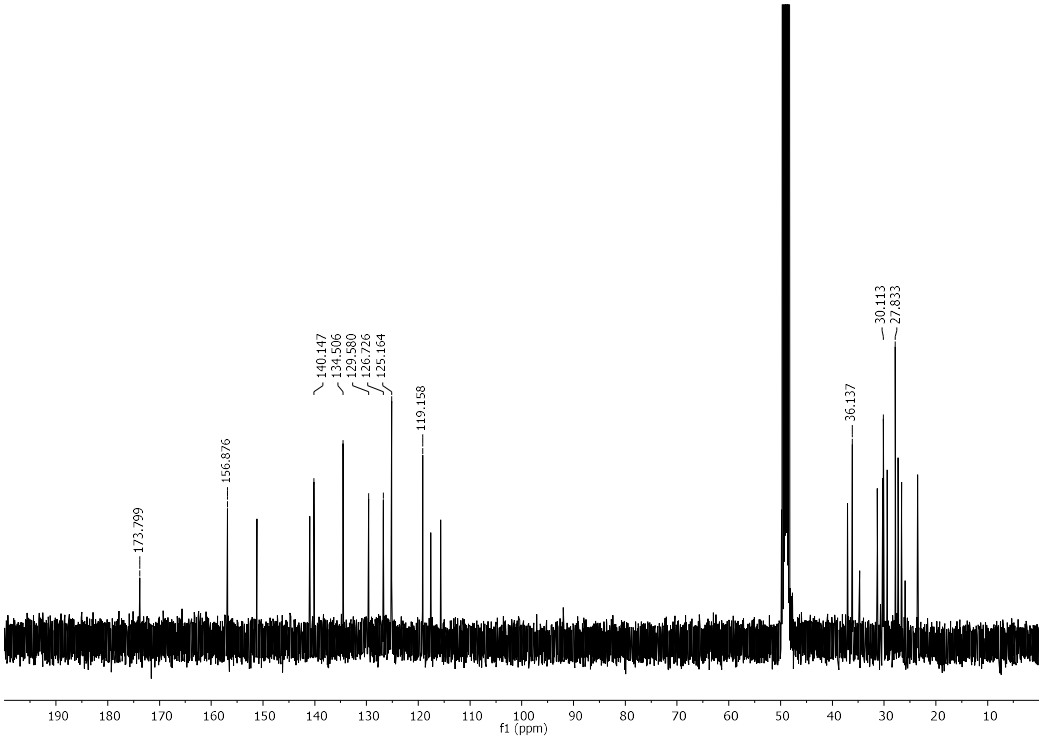
173.799
156.876
140.147
134.506
129.580
126.726
125.164
119.158
36.137
30.113
27.833
190 180 170 160 150 140 130 120 110 100 90 80 70 60 50 40 30 20 10
f1 (ppm)

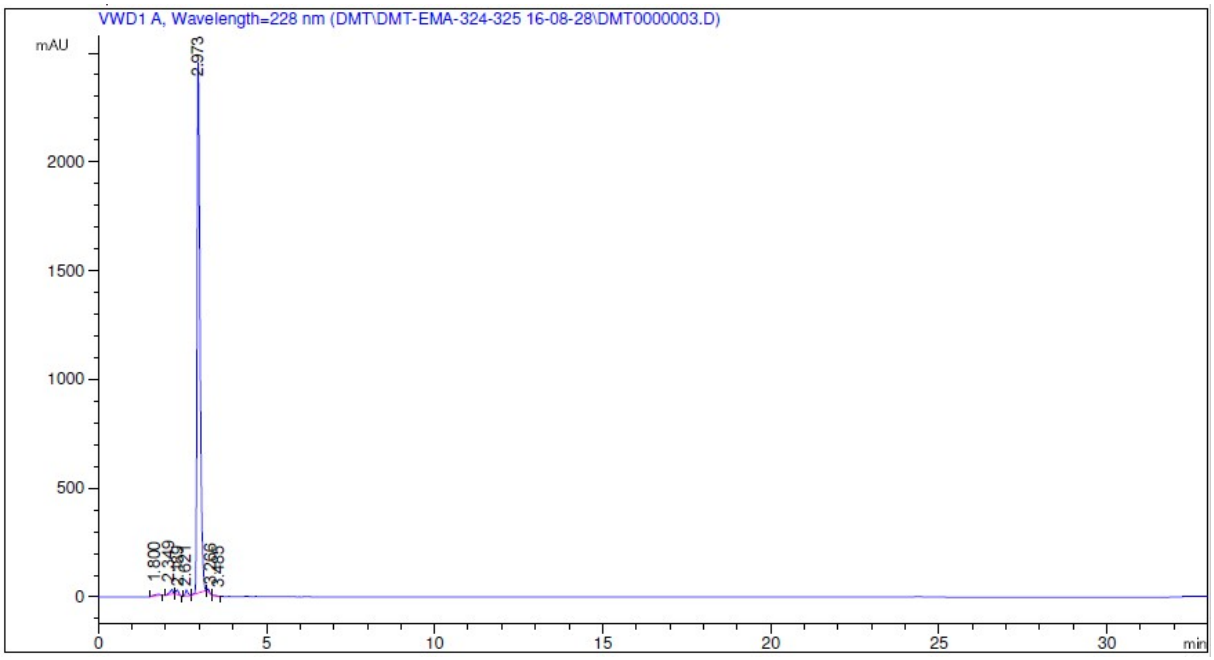
VWD1 A, Wavelength=228 nm (DMT\DMT-EMA-324-325 16-08-28\DMT0000003.D)
mAU
2000
1500
1000
500
0
2.973
1.800
2.349
2.821
3.266
3.485
0 5 10 15 20 25 30 min

4-{9-[(3-Chloro-6,7,10,11-tetrahydro-9-methyl-7,11-methanocycloocta[*b*]quinolin-12-yl)amino]nonanoyl}piperazin-2-one (**13**)

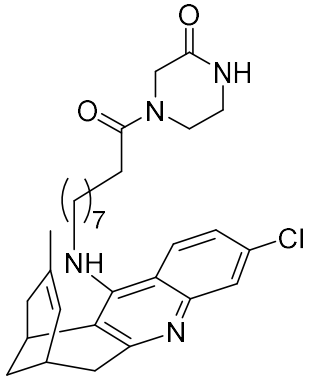

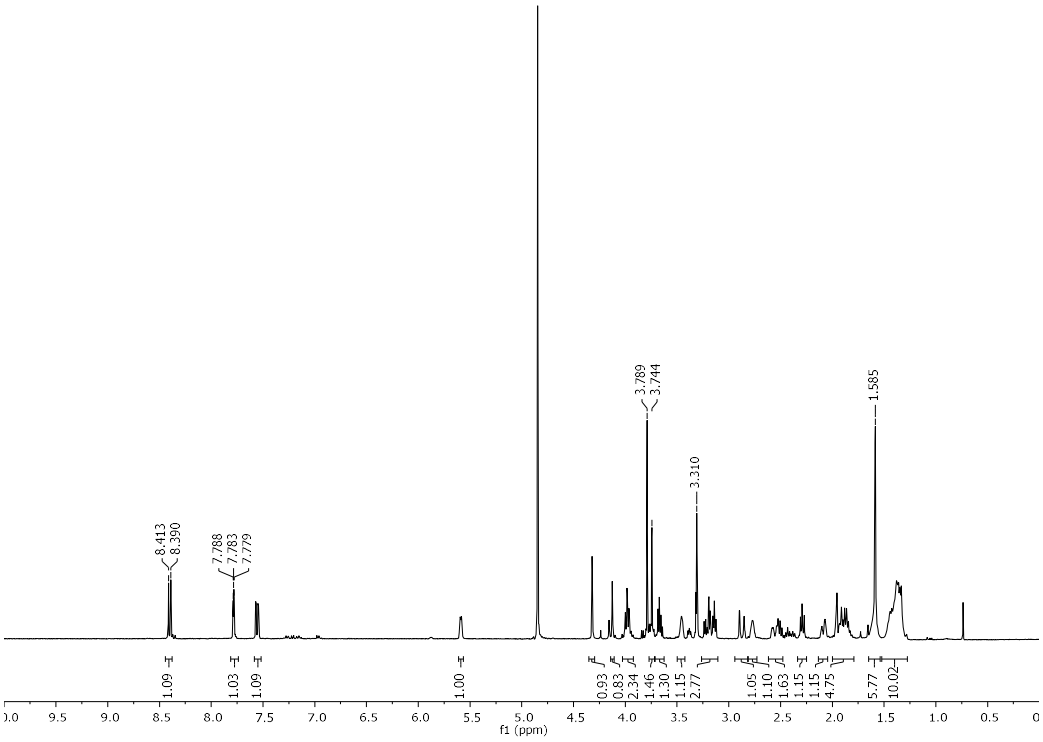

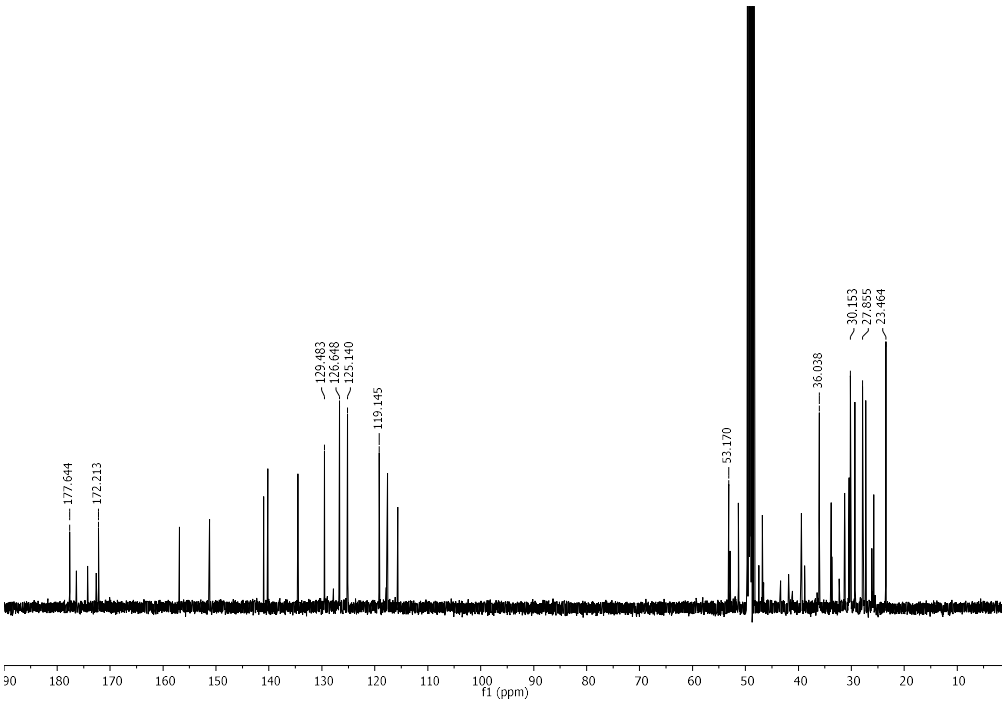
177.644
172.213
129.483
126.648
125.140
119.145
53.170
36.038
30.153
27.855
23.464
f1 (ppm)

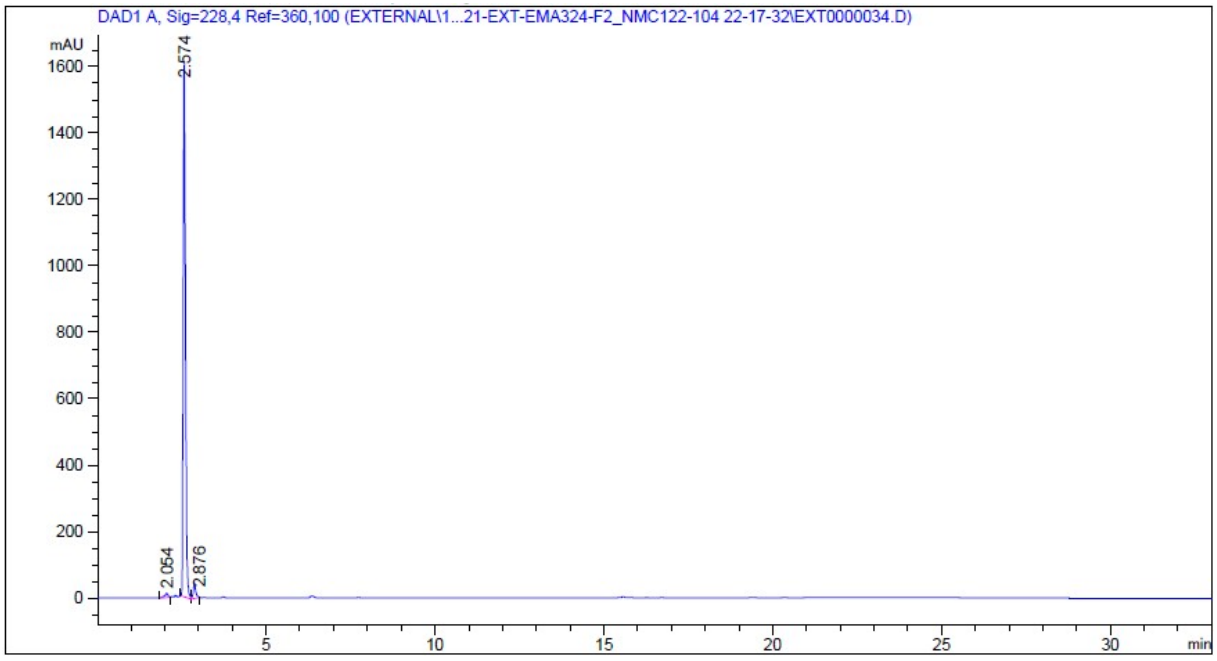
DAD1 A, Sig=228,4 Ref=360,100 (EXTERNAL\1...21-EXT-EMA324-F2_NMC122-104 22-17-32\EXT0000034.D)
mAU
2.574
2.054
2.876
min

9-[(3-Chloro-6,7,10,11-tetrahydro-9-methyl-7,11-methanocycloocta[*b*]quinolin-12-yl)amino]-*N*-[(2-oxo-1,2-dihydro-4-pyridyl)methyl]nonanamide (**14**)

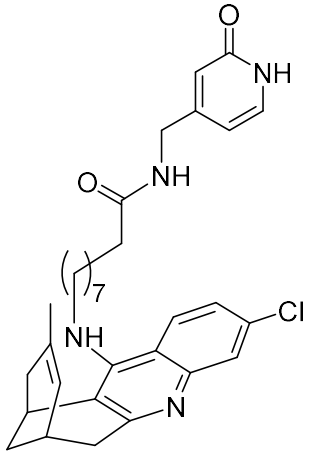

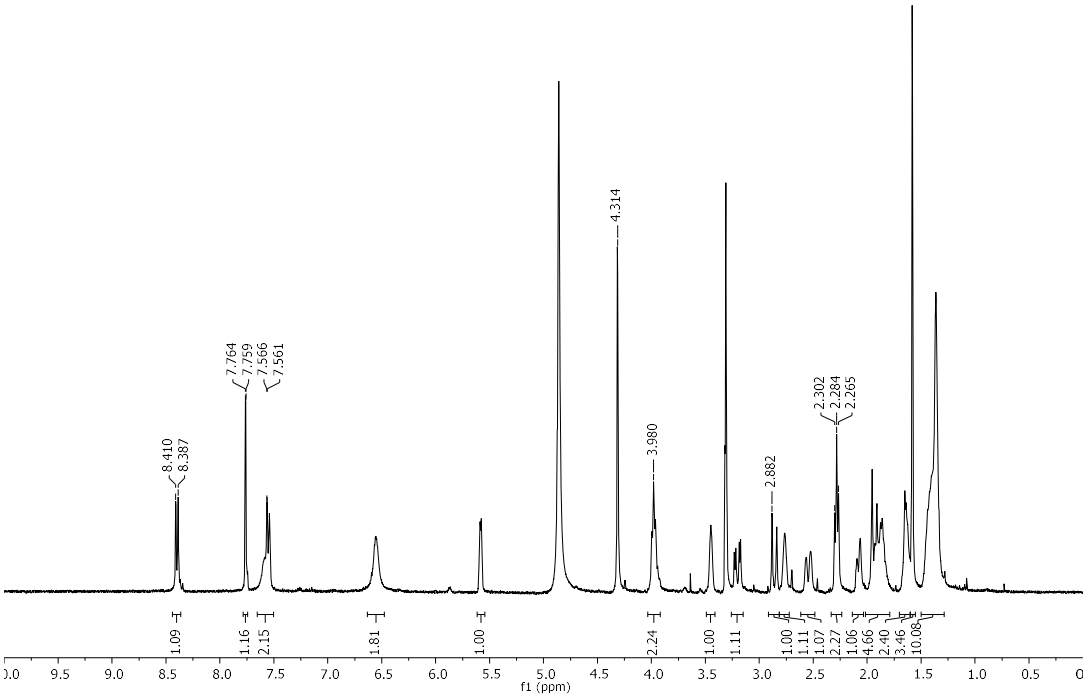

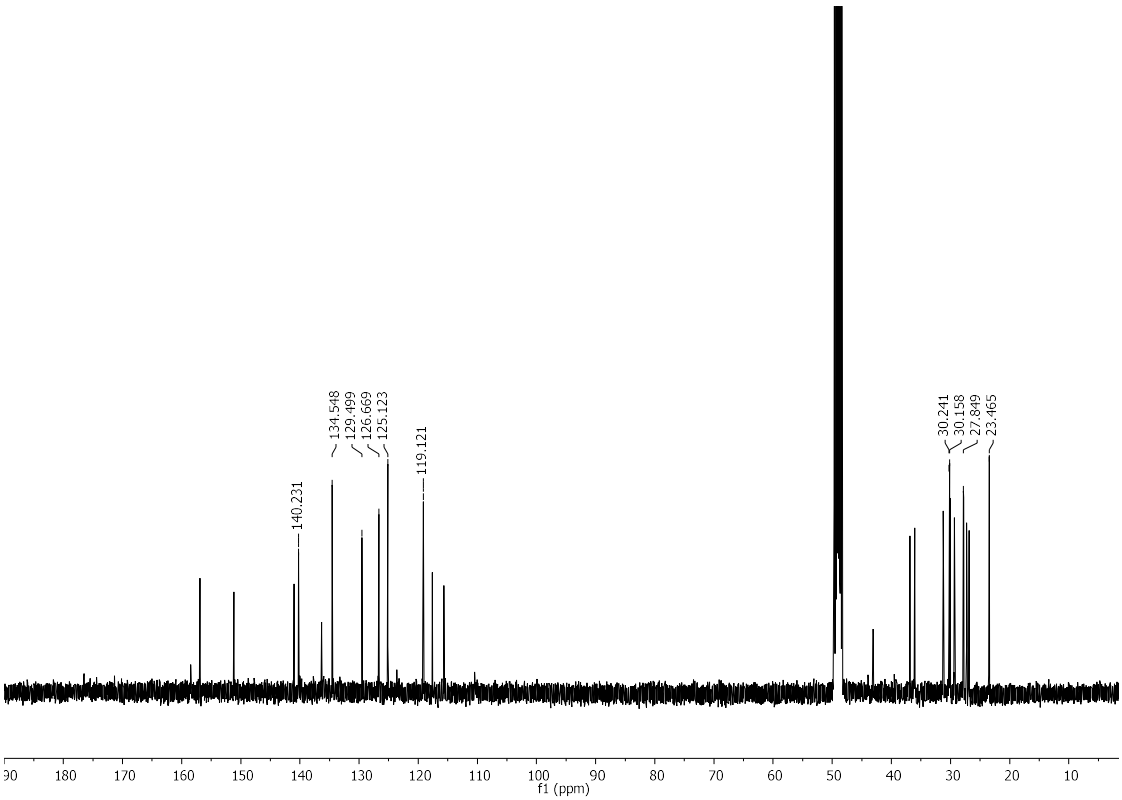
140.231
134.548
129.499
126.669
125.123
119.121
30.241
30.158
27.849
23.465
f1 (ppm)

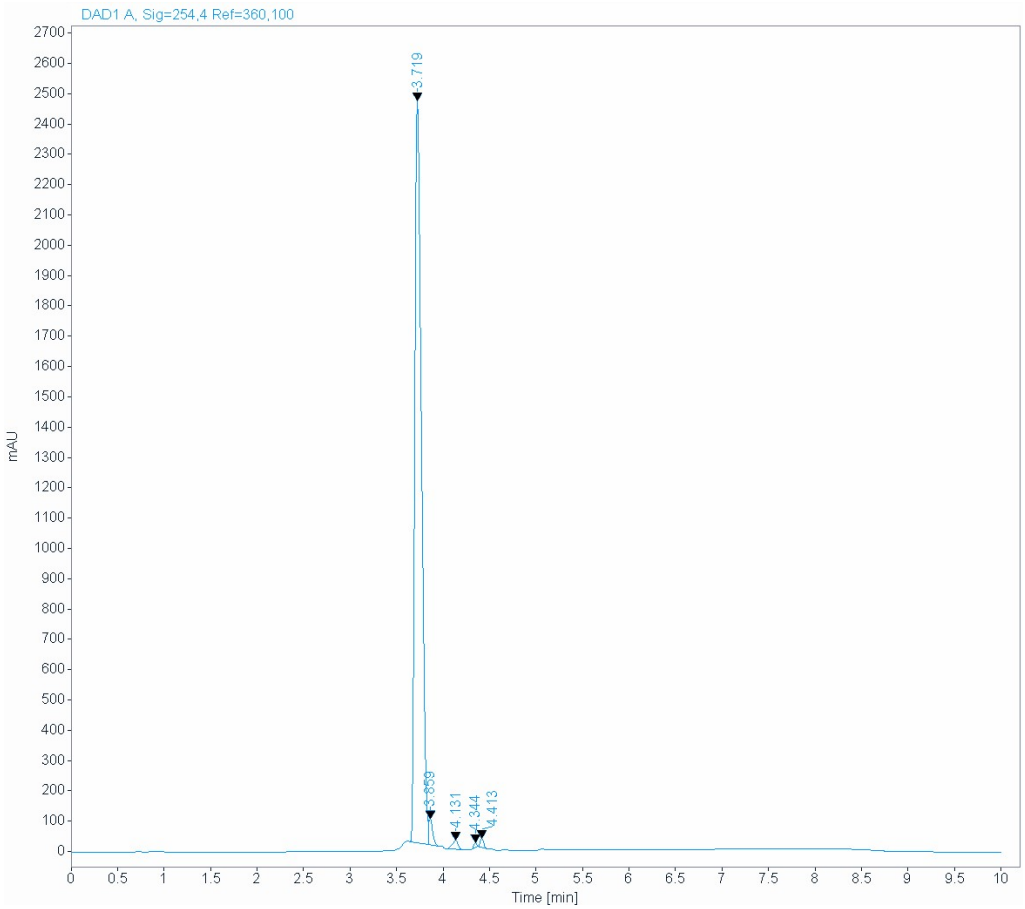
DAD1 A, Sig=254,4 Ref=360,100
mAU
Time [min]
3.719
3.859
4.131
4.344
4.413

9-[(3-Chloro-6,7,10,11-tetrahydro-9-methyl-7,11-methanocycloocta[*b*]quinolin-12-yl)amino]-*N*-[(2-methoxy-4-pyridyl)methyl]nonanamide (**17**)

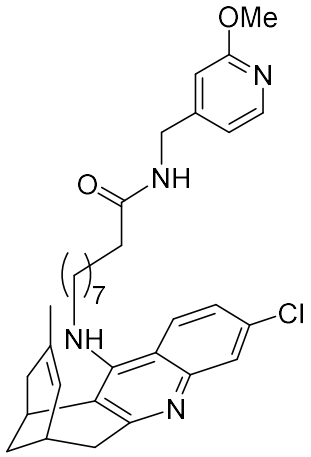

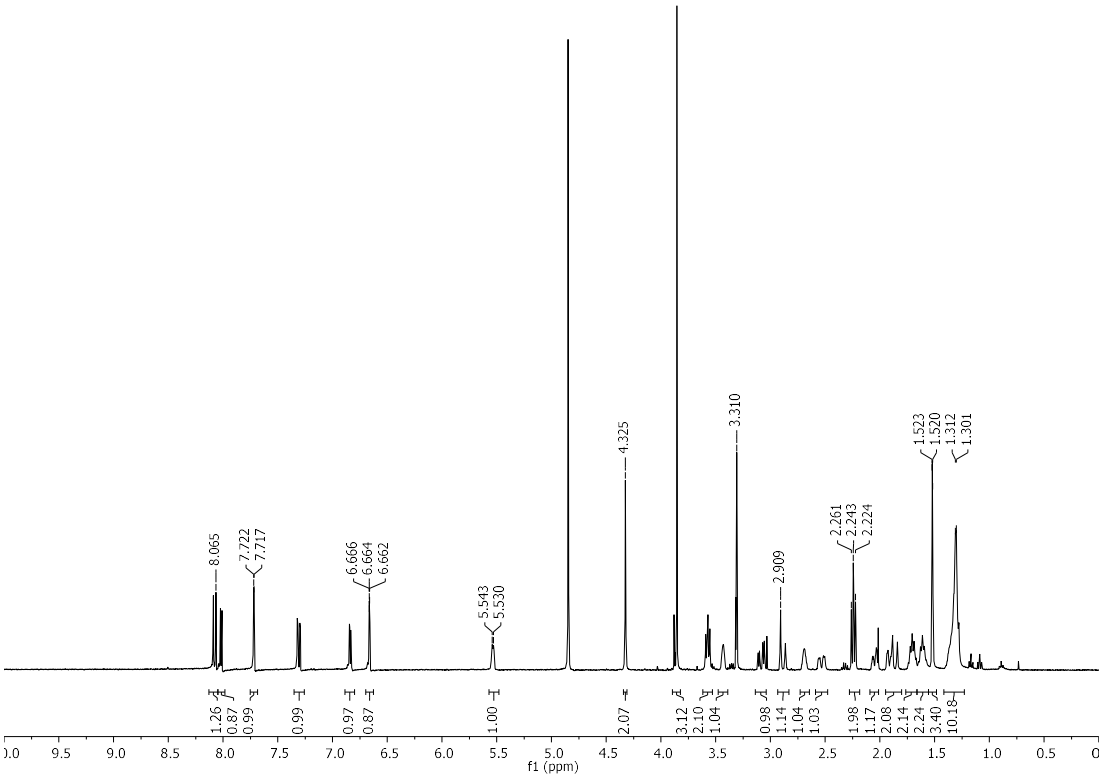

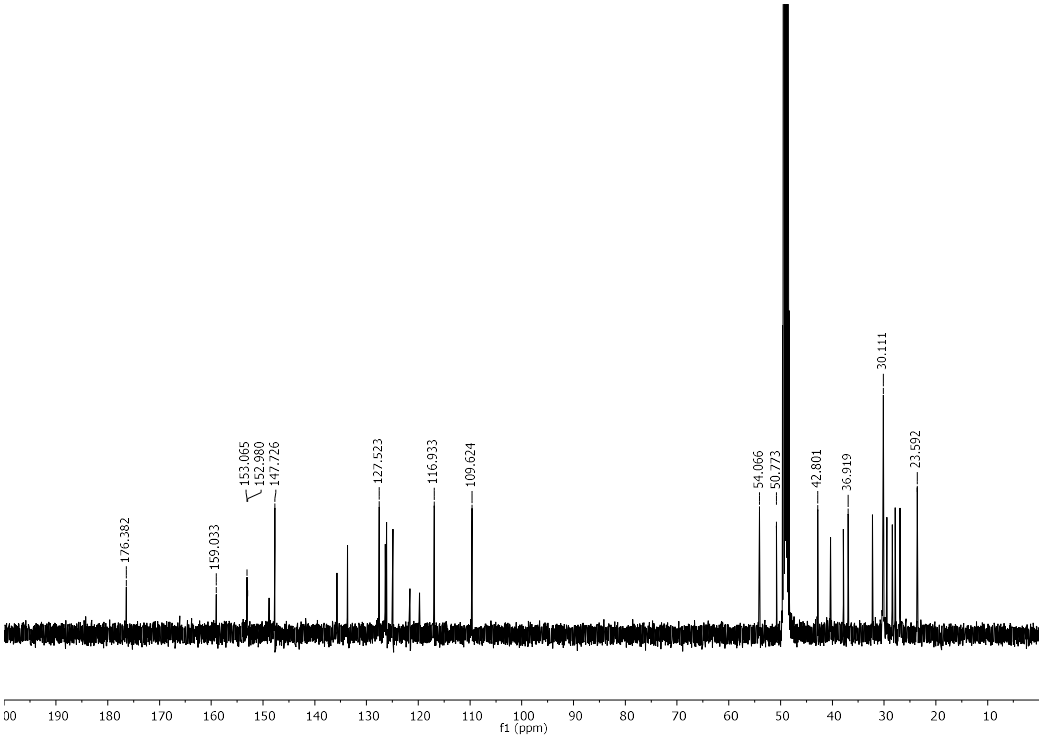
176.382
159.033
153.065
152.980
147.726
127.523
116.933
109.624
54.066
50.773
42.801
36.919
30.111
23.592
f1 (ppm)

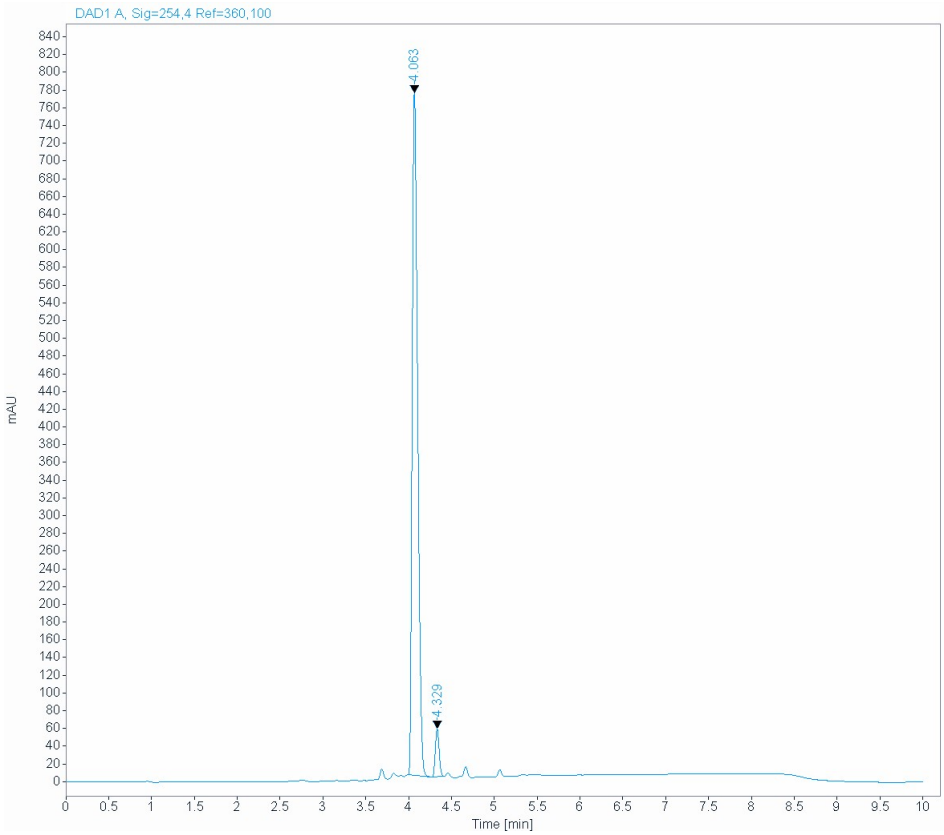
DAD1 A, Sig=254,4 Ref=360,100
mAU
4.063
4.329
Time [min]